Experiments of 0ν $\beta\beta$ Decays

- The present status and the future -

Hideaki Ohsumi
(SAGA)

1. Introduction
2. The detector sensitivities (m_ν limits)
3. Where we are ? Where we should go?
   Histories (the present and the future)
4. Ge detectors
   - Heidelberg-Moscow(GENIUS), IGEX,..
5. Full β-ray tracking experiments
   - ELEGANT, NEMO, ...
6. Thermal Detectors
   - Milano-TeO_2 (CUORE), ...
7. New Directions
   - Liquid scintillators (Xe, LENS(Yb)...)
   - Large scintillater trackers (MOON,...)
   - Others liq. Xe
8. Concluding Remarks

ββ decay of ^{100}Mo

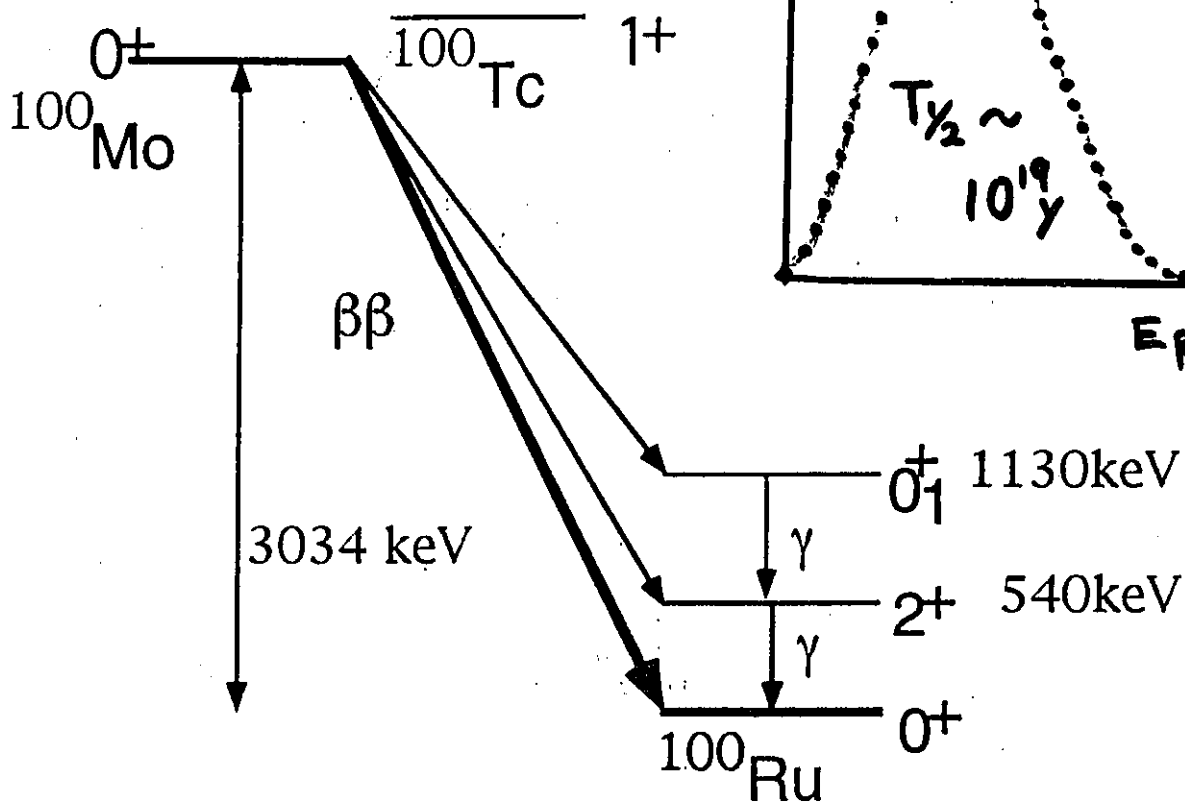

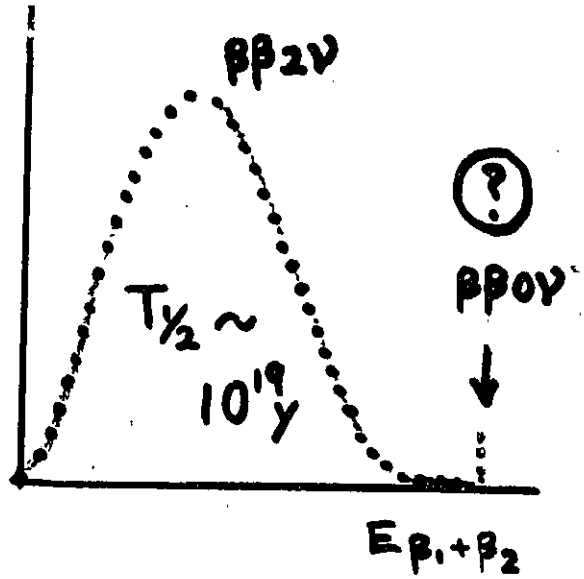

$^{100}Mo \rightarrow {}^{100}Ru + e^- + e^- + (\bar{\nu}) + (\bar{\nu})$

Beyond Standard Model

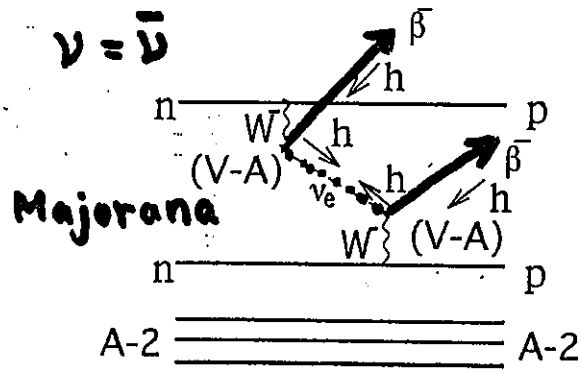

0νββ (mass term)

$\longrightarrow m_\nu$

$\longrightarrow \lambda \sim \left(\frac{M_L}{M_R}\right)^2$

$\eta \sim -\tan\zeta$

M_L, M_R :boson mass

ζ :mixing angl

Within Standard Model

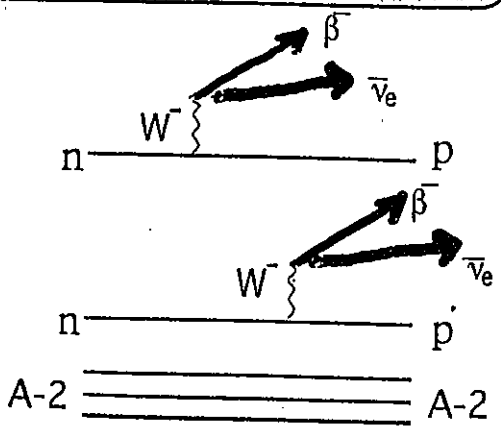

2νββ

Full β-ray tracking

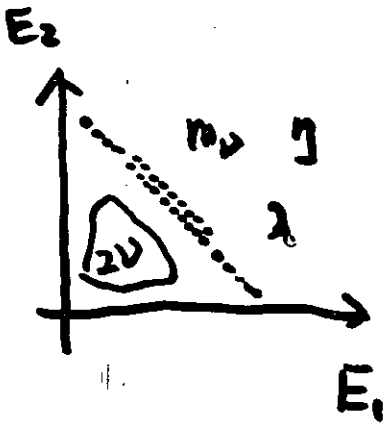

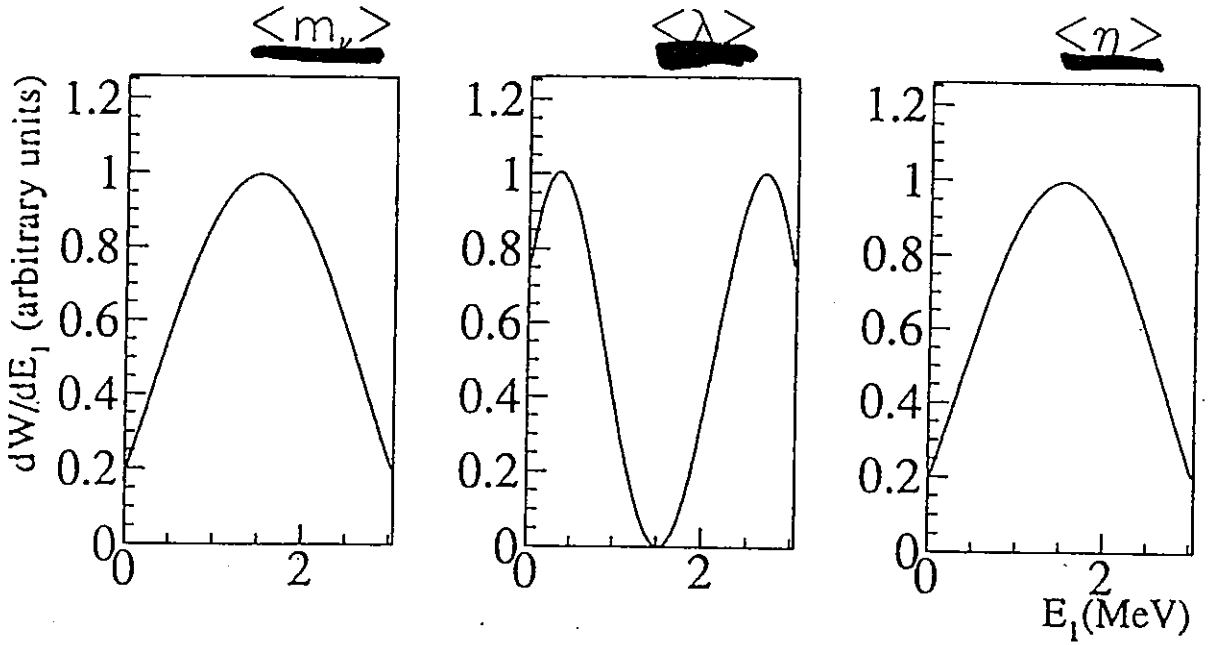

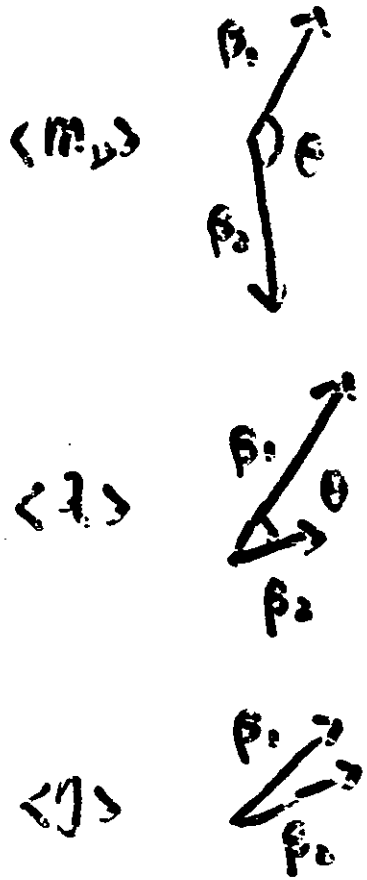

$$\frac{dN}{d\cos\theta} = 1 + \alpha \cos\theta$$

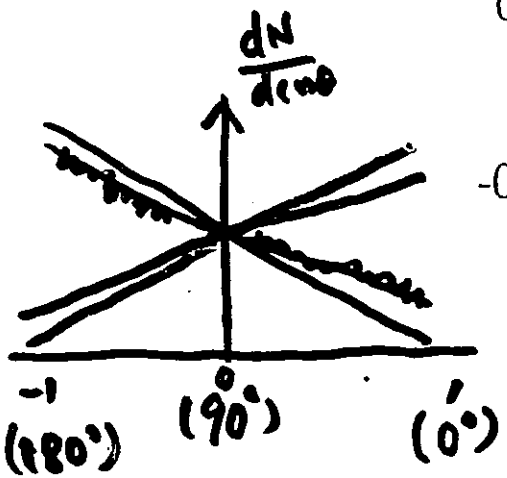

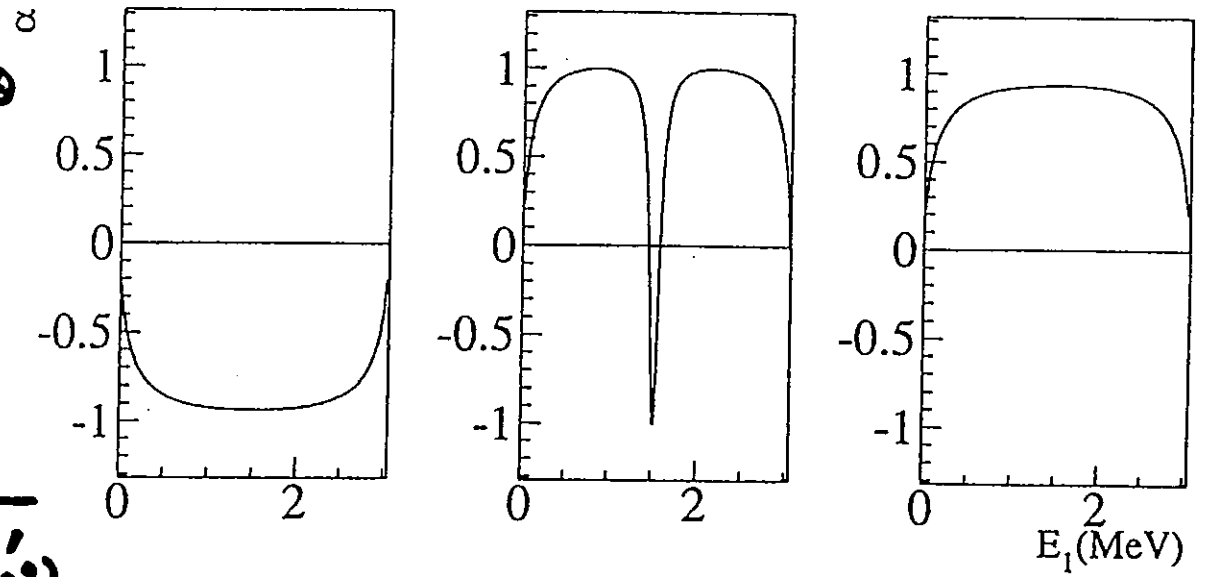

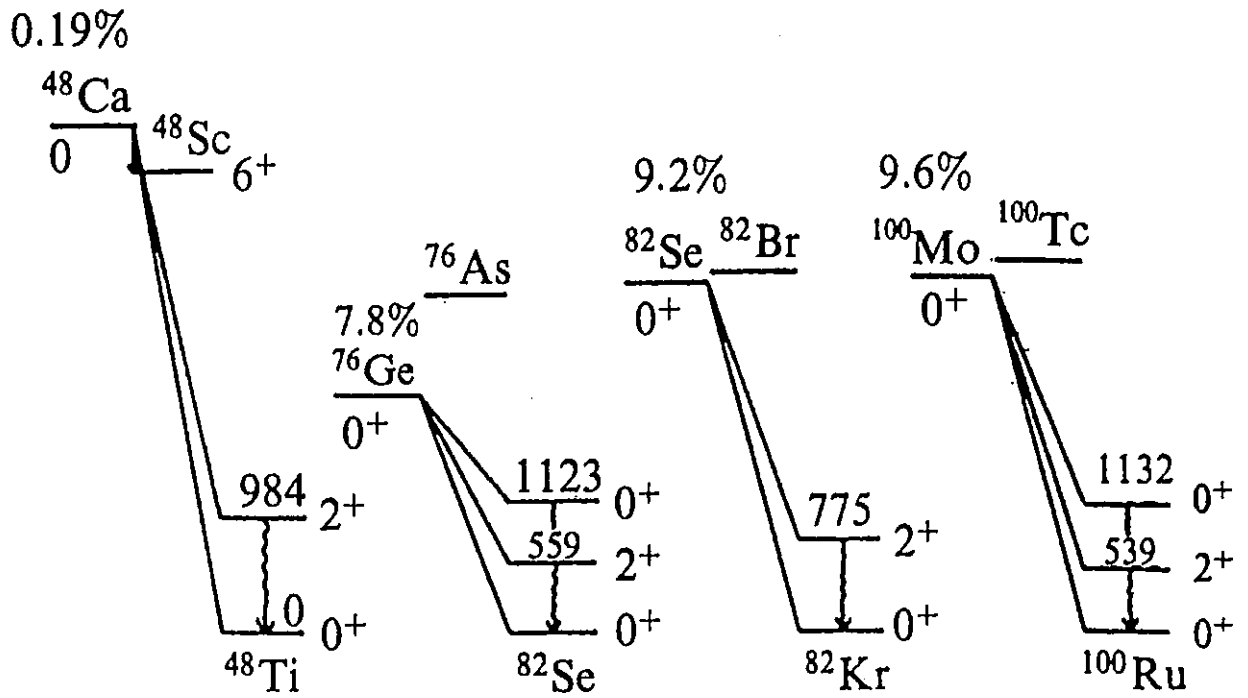

$Q_{\beta\beta}(0^+ \rightarrow 2^+) = 3287\,\text{keV}$	1481	2220	2495
$Q_{\beta\beta}(0^+ \rightarrow 0^+) = 4271\,\text{keV}$	2045	2995	3034

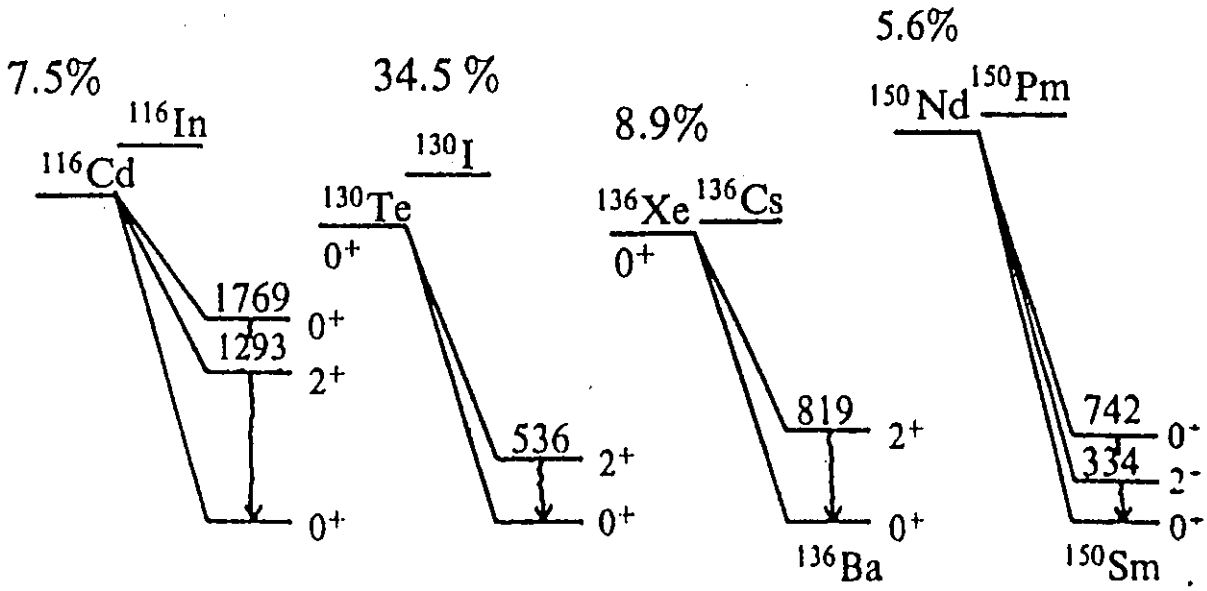

$Q_{\beta\beta}(2^+) = 1509\,\text{keV}$	1997	1660	3033
$Q_{\beta\beta}(0^+) = 2802\,\text{keV}$	2533	2479	3367

Transition	$Q_{\beta\beta}$ (MeV)	$t^{2\nu}_{1/2}$ (yr)	$t^{0\nu\beta\beta}_{1/2}$ (yr)	m_ν (eV) Limits
$^{48}Ca \rightarrow {}^{48}Ti$	4.276		$> 9.5 \times 10^{21}$	
		$4.3(+2.4-1.1 \pm 1.4) \times 10^{19}$		
$^{76}Ge \rightarrow {}^{76}Se$	2.039	$9.2(+0.7-0.4) \times 10^{20}$	$> 0.8 \times 10^{25}$	
		$1.77(\pm 0.01 + 0.13 - 0.11) \times 10^{21}$		
			$> 5.7(1.6^*) \times 10^{25}$	0.24 (0.44*)
$^{82}Se \rightarrow {}^{82}Kr$	2.992	$1.08(+0.26-0.06) \times 10^{20}$	$> 2.7 \times 10^{22}$	5.4
		$0.83(\pm 0.1 \pm 0.07) \times 10^{20}$	$> 9.5 \times 10^{21}$	
$^{96}Zr \rightarrow {}^{96}Mo$	3.351	$3.9(\pm 0.9) \times 10^{19}$		
		$2.1(+0.8-0.4 \pm 0.2) \times 10^{19}$	$> 1.0 \times 10^{21}$	
$^{100}Mo \rightarrow {}^{100}Ru$	3.034	$1.15(+0.3-0.2) \times 10^{19}$	$> 8.2 \times 10^{22}$	1.8
		$6.82(+0.38-0.53 \pm 0.68) \times 10^{18}$	$> 1.23 \times 10^{21}$	
		$7.6(+2.2-1.4) \times 10^{18}$	$> 2.2 \times 10^{22}$	
$^{116}Cd \rightarrow {}^{116}Sn$	2.804	$2.6(+0.9-0.5 \pm 0.35) \times 10^{19}$	$> 5.4 \times 10^{21}$	
		$2.7(+0.5-0.4+0.9-0.6) \times 10^{19}$	$> 2.9 \times 10^{22}$	
		$3.6(\pm 0.35 \pm 0.21) \times 10^{19}$	$> 5.0 \times 10^{21}$	
$^{128}Te \rightarrow {}^{128}Xe$	0.867	$7.7(\pm 0.4) \times 10^{24}$	$> 6.9 \times 10^{24}$	
$^{130}Te \rightarrow {}^{130}Xe$	2.529	$2.7(\pm 0.1) \times 10^{21}$	$> 2.5 \times 10^{21}$	
			$> 5.6 \times 10^{22}$	4.1
$^{136}Xe \rightarrow {}^{136}Ba$	2.467	$> 3.6 \times 10^{20}$	$> 4.4 \times 10^{23}$	3.5
$^{150}Nd \rightarrow {}^{150}Sm$	3.368	$6.75(+0.37-0.42 \pm 0.68) \times 10^{18}$	$> 1.22 \times 10^{21}$	7.1
$^{238}U \rightarrow {}^{238}Pu$	1.437	$2.0(\pm 0.6) \times 10^{21}$	$> 0.8 \times 10^{21}$	
$^{244}Pu \rightarrow {}^{244}Cm$	1.352	$> 1.1 \times 10^{18}$	$> 1.1 \times 10^{18}$	

The Detector Sensitivities

- m_ν limits VS Experimental parameters -

- Transition probabilities

$$\Gamma \equiv \frac{\ln 2}{T_{1/2}} = S_n \cdot m_\nu^2 \qquad S_n = G^{0\nu}|M^{0\nu}|^2 \ \propto Q_{\beta\beta}^5$$

- The numbers of 0ν $\beta\beta$ events

$$Y_s = n_0 \cdot \Gamma \cdot \epsilon_D \cdot t_m$$

○ Y_{BG} (# of background events) ~ 0

$$Y_s < 1 \Longrightarrow m_\nu < n_0^{-1/2} t_m^{-1/2} S_n^{-1/2} \epsilon_D^{-1/2}$$

○ $Y_{BG} \gg 0$ $\qquad (Y_{BG}{=}\Delta E \cdot I_{BG})$ t_m)

$$Y_s < \sqrt{Y_{BG}} \Longrightarrow m_\nu < n_0^{-1/2} t_m^{-1/4} S_n^{-1/2} \epsilon_D^{-1/2} (\Delta E \cdot I_{BG})^{1/4}$$

○ $Y_{BG} \propto n_0$ $\qquad (I_{BG} = n_0 \cdot K_{BG})$

$$\Longrightarrow m_\nu < n_0^{-1/4} t_m^{-1/4} S_n^{-1/2} \epsilon_D^{-1/2} (\Delta E \cdot K_{BG})^{1/4}$$

n_0: # of $\beta\beta$ source, t_m: Measuring time
ϵ_D: Detector efficiency, ΔE: Energy resolution

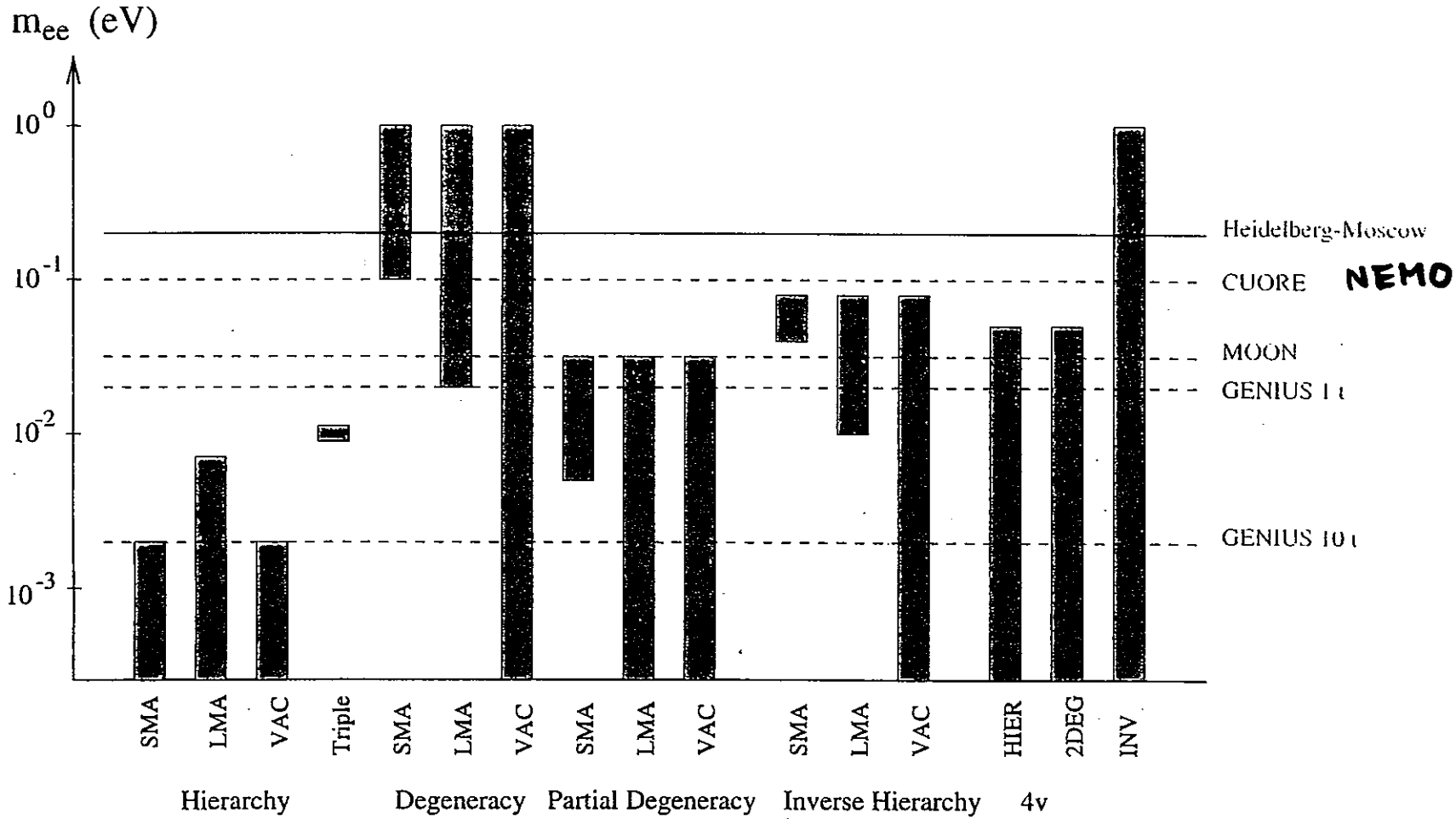

Figure 26: Summary of expected values for m_{ee} in the different schemes discussed in this paper. The expectations are compared with the recent neutrino mass limits obtained from the Heidelberg–Moscoscow [44] experiment as well as the expected sensitivities for the CUORE [56], MOON [57] proposals and the 1 ton and 10 ton proposal of GENIUS [13].

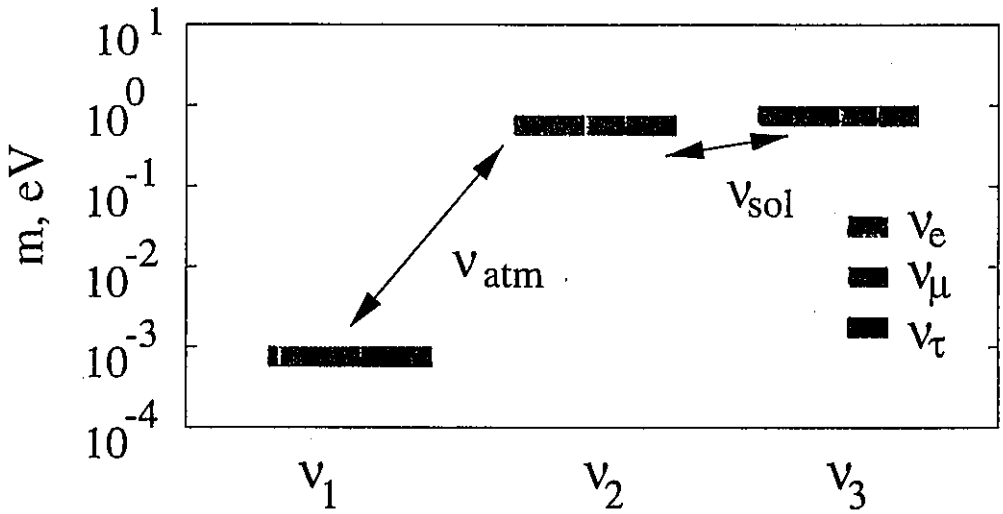

Figure 11. Neutrino masses and mixings in the scheme with inverse hierarchy. Shown is the example with large solar neutrino mixing.

m_ν	1 eV	0.1 eV	0.01 eV	0.001 eV
n_0	6×10^{23}	6×10^{25}	6×10^{27}	6×10^{29}
	(100g)	(10kg)	(1 t)	(100 t)
$T_{1/2}$	10^{23}y	10^{25}y	10^{27}y	10^{29}y

^{76}Ge
- Heidelberg-Moscow → GENIUS →
- IGEX

β-ray tracking
- NEMO2 → NEMO3
- ELEGANT V - - - → MOON →
- UCI-TPC(Se)
- Neuchatel (Xe)
- DCBA(Nd) →

Borometer
- Milano-TeO_2 → CUORICINO → CUORE →

liquid scintillator
- CTF(Xe) → BOREX(Xe) →
- LENS(Yb) →
- CAMEO I → CAMEO II → CAMEO III →

others
- CaF_2 (Osaka, etc) →
- liquid-Xe →

Ge Detectors

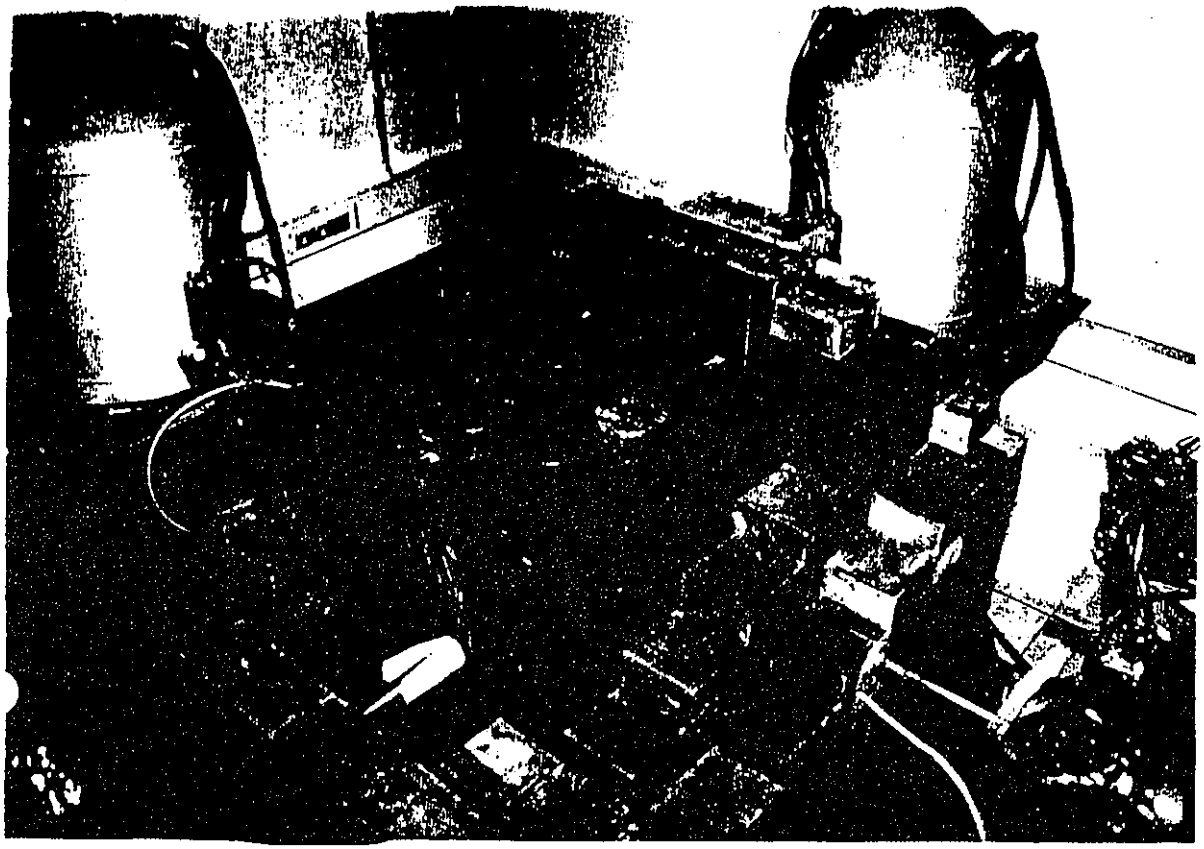

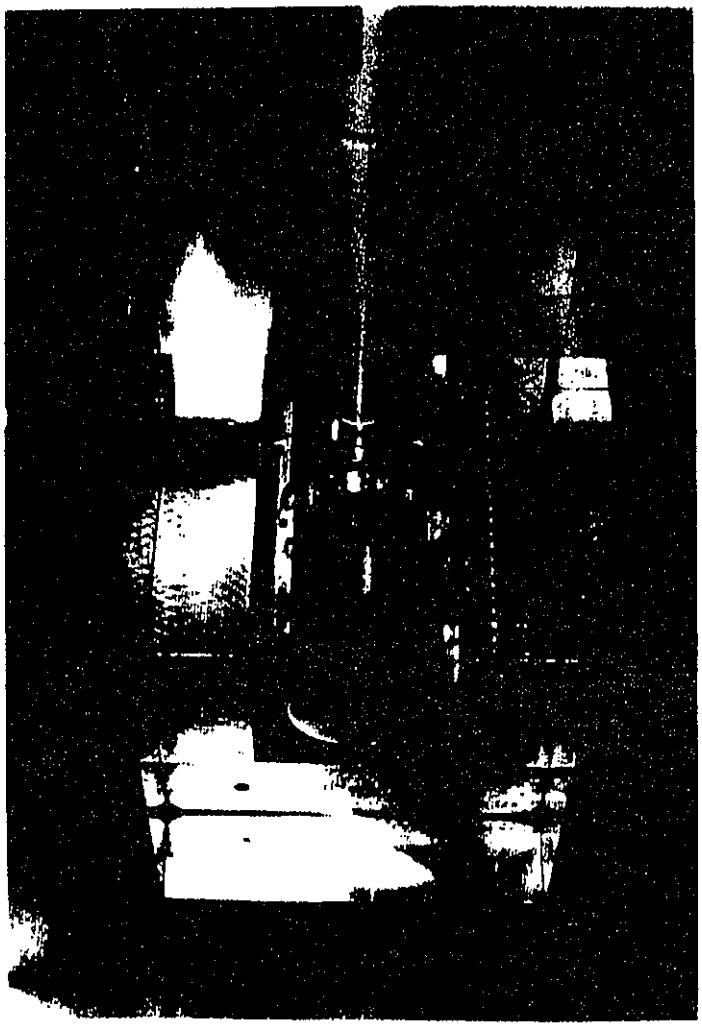

Figure 6.36. Top and lower left: the first five enriched "high-purity" ^{76}Ge detectors in the world, in the Heidelberg–Moscow $\beta\beta$ setup (shielded by low-level lead and electrolytic copper) in the Gran Sasso (photos: B. Maier). Lower right: an enriched 3.5 kg ^{76}Ge crystal before conversion into a 2.9 kg detector (photo: MPI Heidelberg).

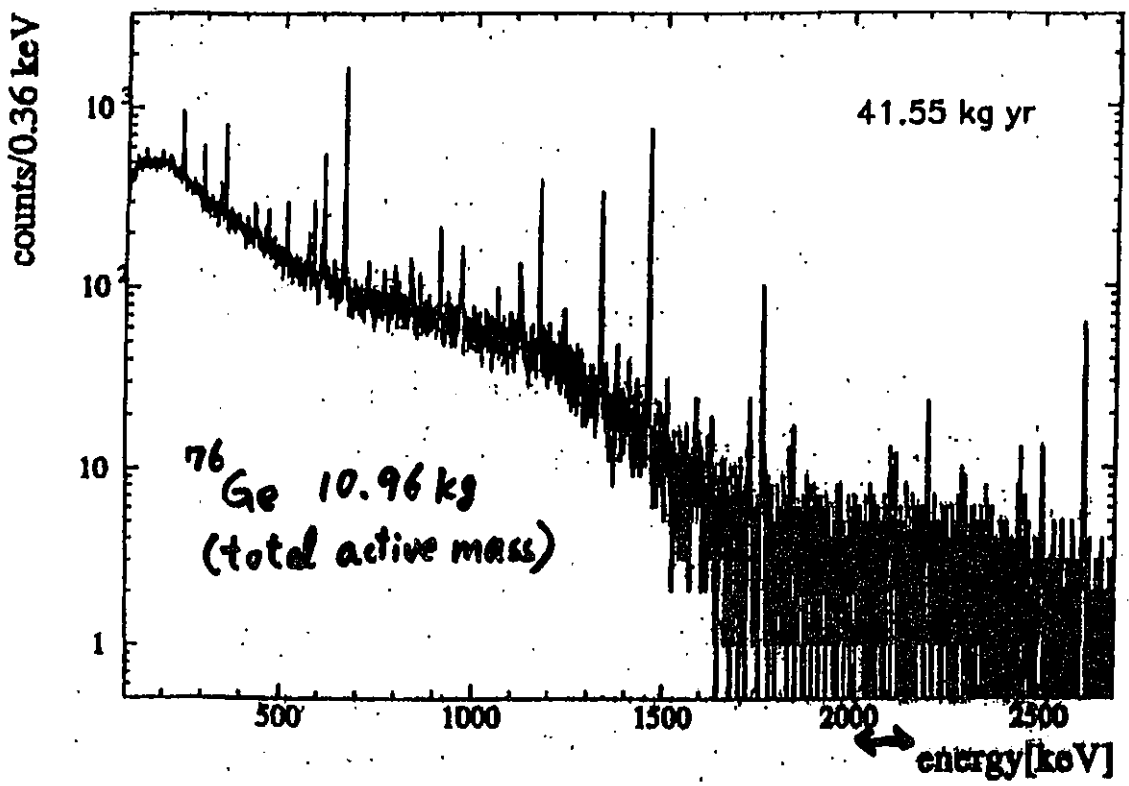

FIG. 1. Sum spectrum of all detectors of the Heidelberg-Moscow experiment with 41.55 kg yr for the energy region between 100 and 2700 keV.

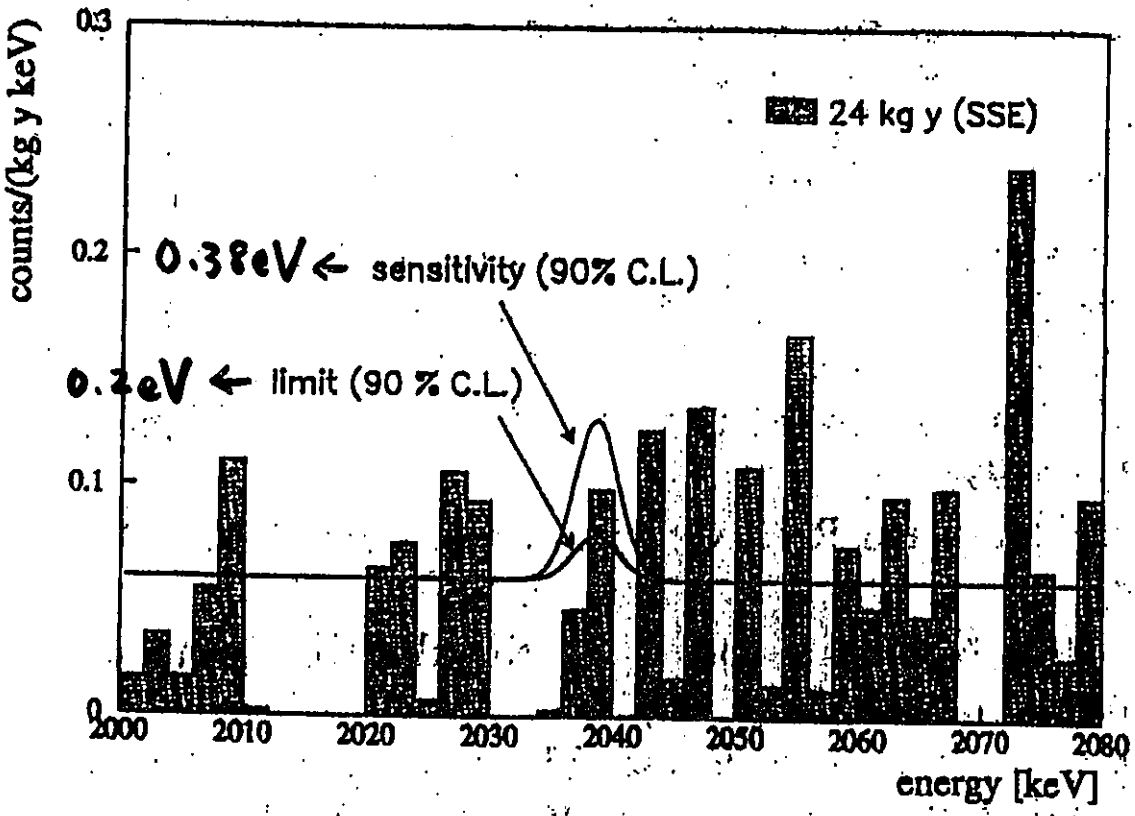

FIG. 3. SSE spectrum after 24.16 kg yr and the corresponding excluded signal and sensitivity of the experiment, at 90% C.L. after [10]. (Particle Data Group (PDG98) ← (PDG96))

@ Canfranc Underground Lab.

Spanish Pyrenees

2450mwe

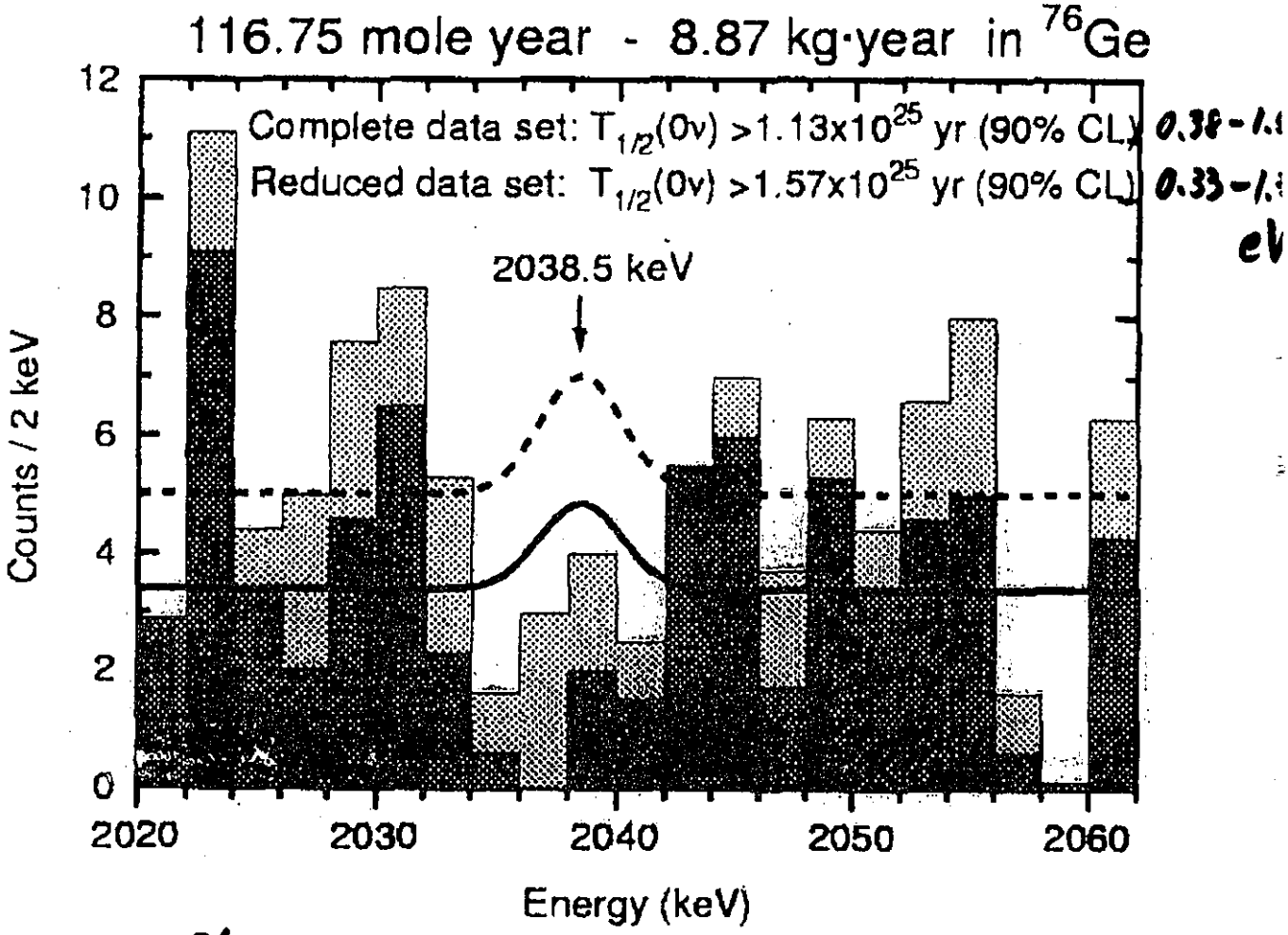

^{76}Ge ... 3 x 2kg

Figure 1. IGEX data sets and $0\nu\beta\beta$ signal excluded with and without application of PSD.

Multi Sector Event

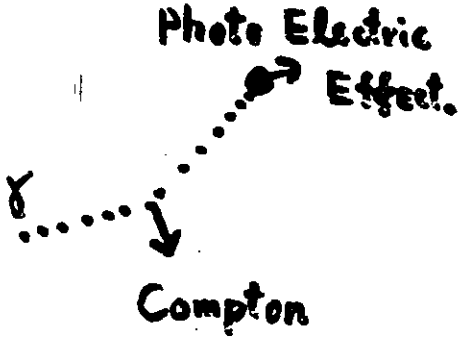

Single Sector Event

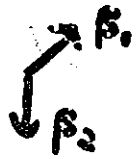

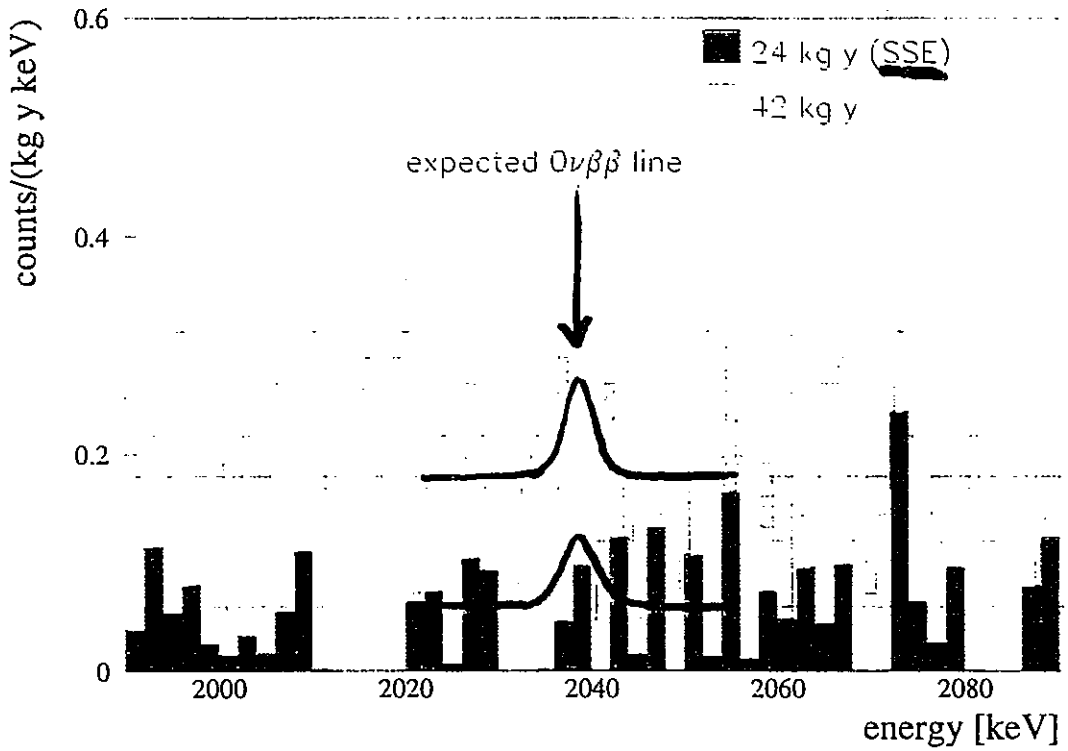

Fig. 13 *Integral spectrum in the region of interest after subtraction of the first 200 days of measurement of each detector, leaving 42 kg y of measuring time. The darkened histogram corresponds to data accumulated meanwhile using a new pulse shape analysis method (SSE) [Hel96] in a measuring time of 24 kg y. The two solid curves correspond to the signal excluded with 90%C.L. (by the 42 kg y measurement and the 24 kg y SSE measurement). They correspond to* $T_{1/2}^{0\nu} > 1.3 \cdot 10^{25}$ *y (upper curve) and* $T_{1/2}^{0\nu} > 1.6 \cdot 10^{25}$ *y, respectively.*

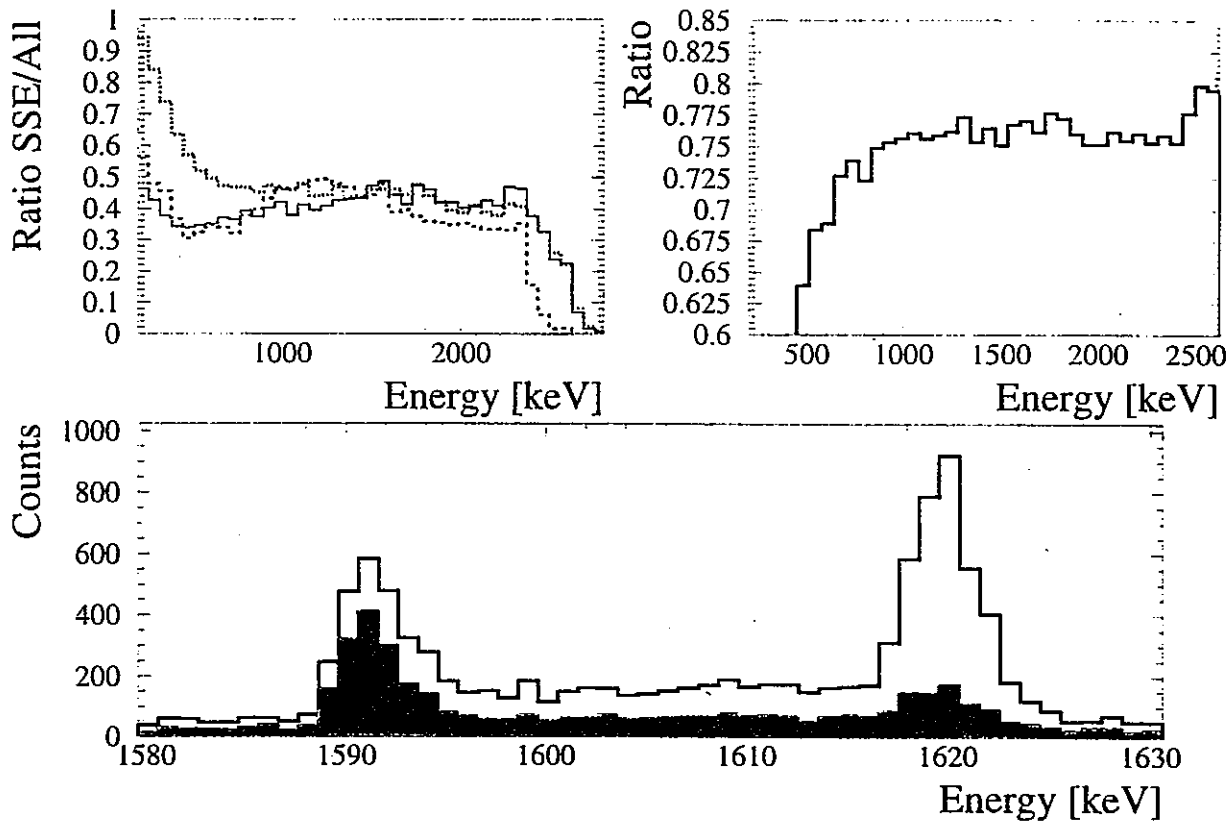

Fig. 4. Upper Panel left: Fraction of SSE's in the spectrum obtained using Neural Network (solid line), applying the one-parameter cut (densely dashed line) and the expectation from the simulation (losely dashed line). Upper panel right: Fraction of pulses identified identically by Neural Network and one-parameter cut. Lower panel: Measured spectrum in the energy region of the reference pulses (data independent of the training sample). The filled histogram corresponds to the identified SSE pulses. The open histogram shows the spectrum of all events.

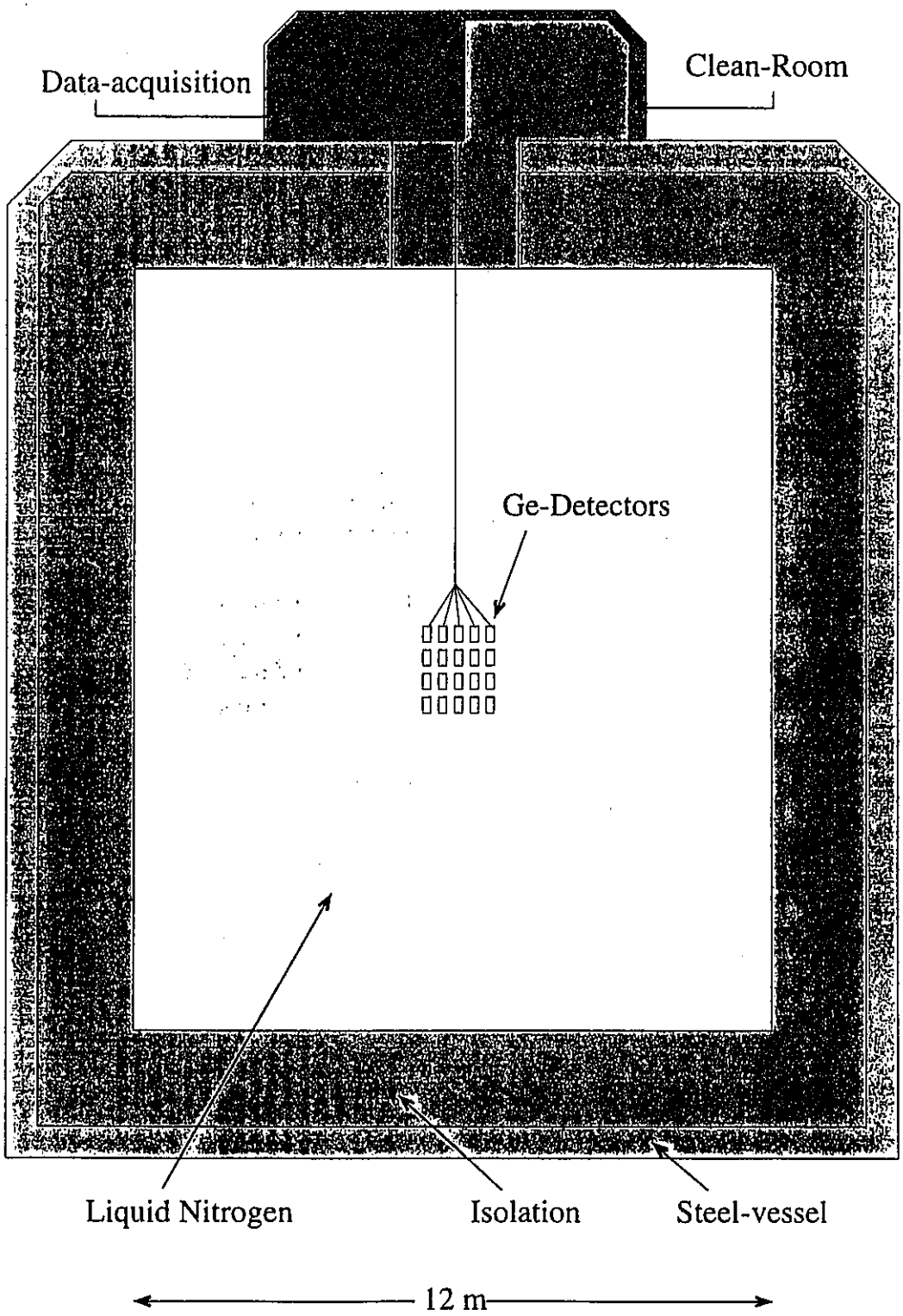

GENIUS $^{76}Ge \sim 1$ ton

(288 enriched ^{76}Ge detectors)

10 years measurments

$T_{1/2}^{0\nu} \geq 6.4 \cdot 10^{28} y$

$m_\nu \leq 0.006 eV$

if ^{76}Ge 10ton

$T_{1/2} \geq 5.7 \cdot 10^{29} y$

$m_\nu \leq 0.002$ eV

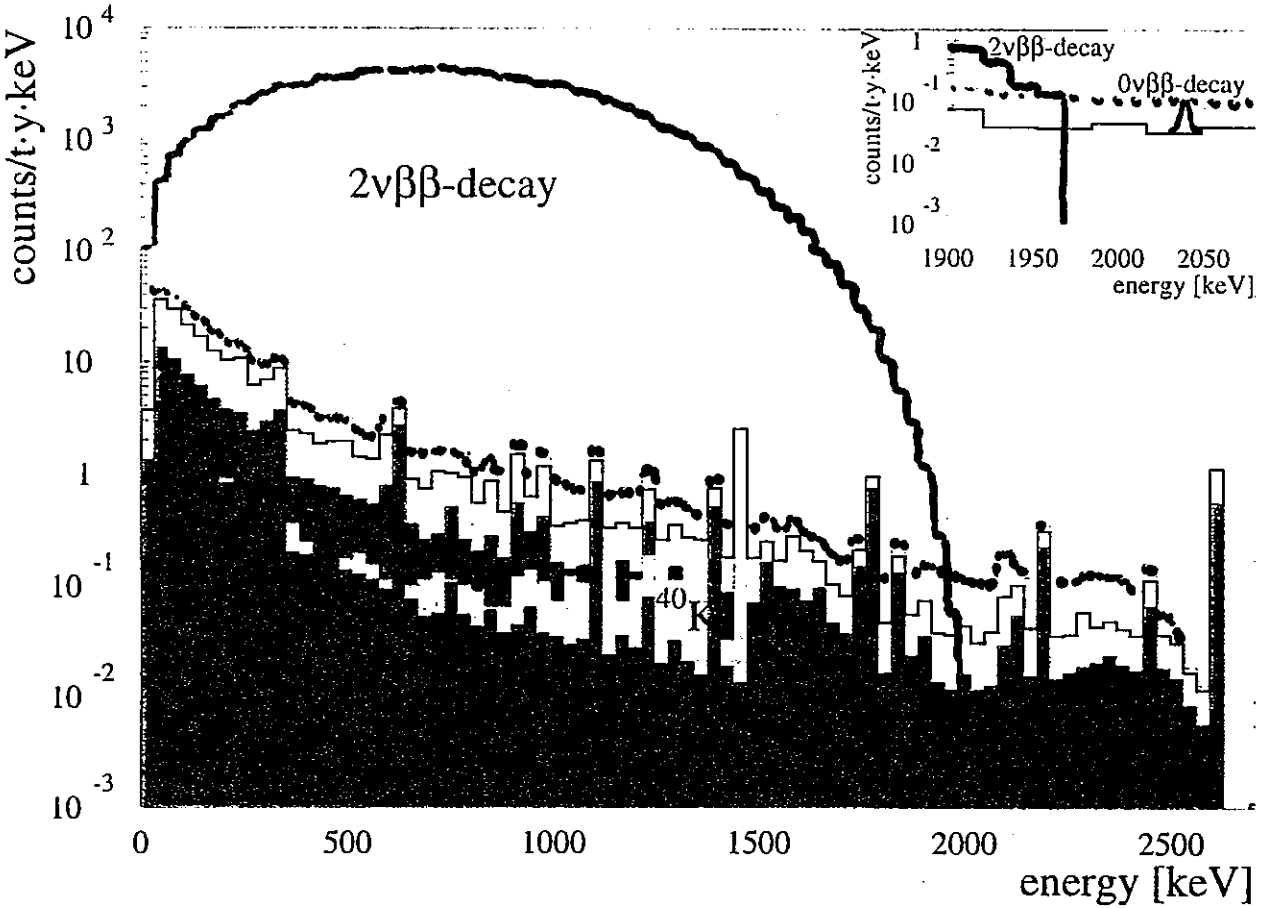

Fig. 18

Monte Carlo simulation of the background of GENIUS. Simulations of U/Ra, U/Th and ^{40}K (shaded), ^{222}Rn (black histogram) activities in the liquid nitrogen; the sum of the activities is shown with anticoincidence between the 288 detectors (thick line) and without (dashed line); the $2\nu\beta\beta$-decay dominates the spectrum with 4 million events per year (from [Kla98c]).

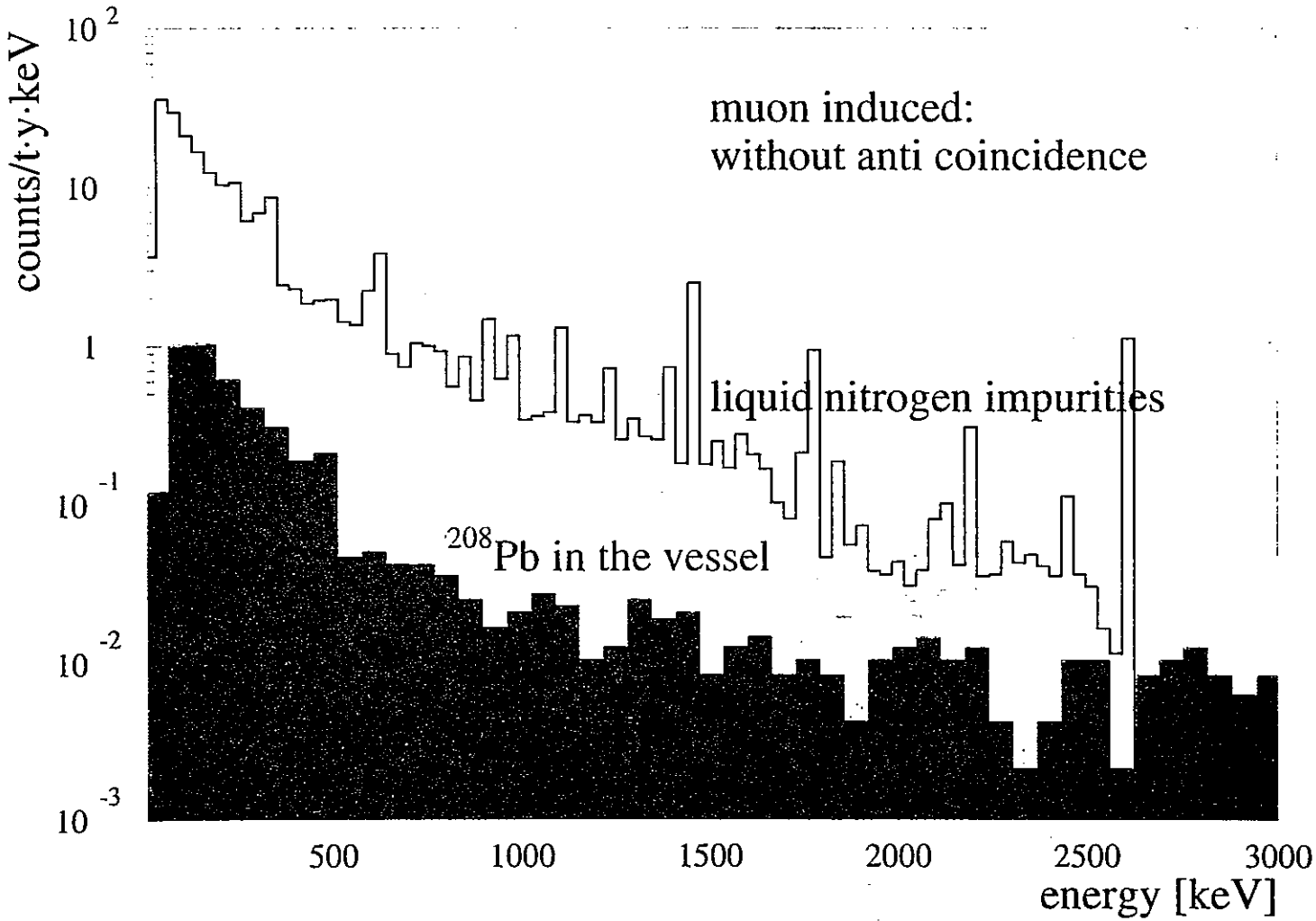

Fig. 19

Background from outside the nitrogen: 200 GeV muons induced events (dashed line) and single hit events (filled histogram); decay of ^{208}Tl in the steel vessel (light shaded histogram) and the background originating from the nitrogen impurities for comparison (thick line) (from [Kla98c])

The NEMO3 detector

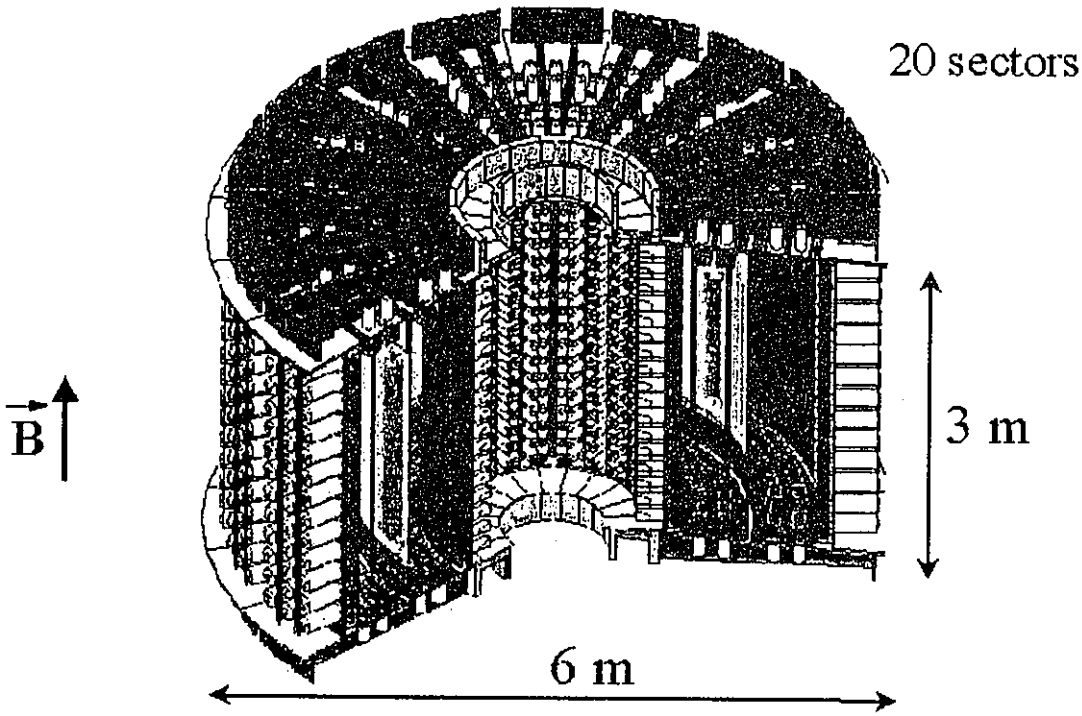

Source : 10 kg of ββ isotopes (20 m² with 50 μm thickness)

Tracking : 6180 Geiger cells

Calorimeter : 1940 plastic scintillators coupled to low radioactivity PM
ΔE/E (FWHM) at 1 MeV: walls 13%; top & bottom 14.5%

Magnetic field : 30 Gauss

Shielding : Iron (20 cm) + neutron shielding

Identification : e^-, e^+, γ, α

ββ events detection

Measurement of source radiopurity

Background rejection

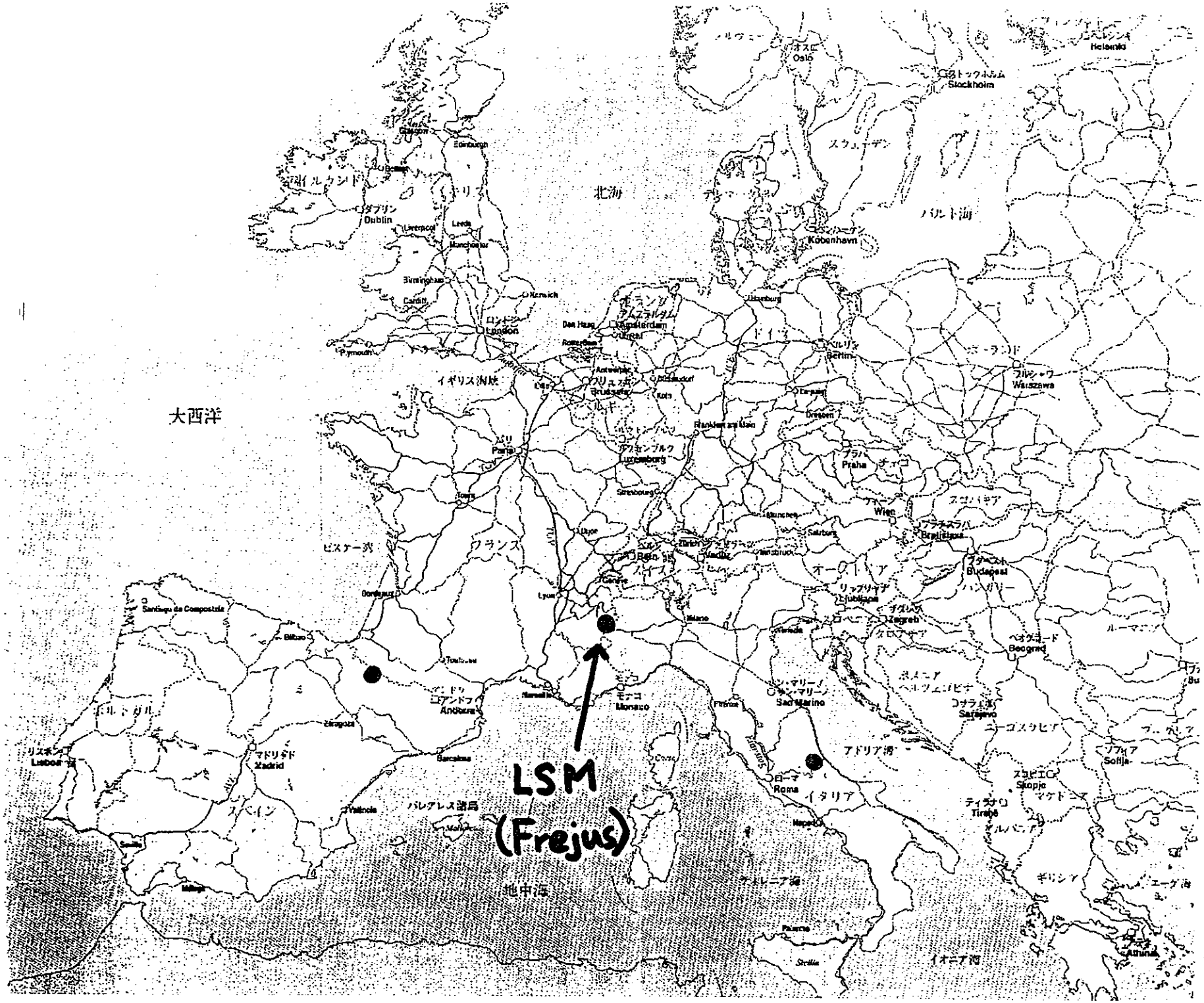
大西洋
北海
バルト海
イギリス海峡
ビスケー湾
地中海
アドリア海
イオニア海
LSM
(Frejus)
Dublin
London
Paris
Bruxelles
Luxembourg
Amsterdam
Berlin
Warszawa
Praha
Wien
Bratislava
Budapest
Zagreb
Beograd
Sarajevo
Sofija
Skopje
Tirana
Athina
Roma
Milano
Lyon
Marseille
Monaco
Andorra
Barcelona
Madrid
Lisboa
Bilbao
Toulouse
Bordeaux
Zürich
München
Salzburg
Ljubljana
Oslo
Stockholm
Helsinki
København
Hamburg
Frankfurt am Main
Köln
Dresden
Strasbourg
Genève
Valencia
Palermo
Napoli
Milano
Venezia
Genova
Torino
Nice
Cannes
Dijon
Rouen
Le Havre
Caen
Brest
Nantes
Rennes
Tours
Orléans
Clermont-Ferrand
Limoges
Poitiers
Angers
Lille
Reims
Metz
Nancy
Mulhouse
Bern
Basel
Innsbruck
Graz
Salzburg
Linz
Klagenfurt
Bologna
Firenze
Pisa
Genova
Torino
Milano
Bergamo
Brescia
Verona
Padova
Trieste
Udine
Bari
Brindisi
Taranto
Catania
Messina
Palermo
Cagliari
Sassari
Zaragoza
Valencia
Sevilla
Málaga
Granada
Murcia
Alicante
Santiago de Compostela
Porto
Coimbra
Évora
Faro
Ponta Delgada
Funchal
Las Palmas
Santa Cruz de Tenerife
Palma de Mallorca
Ibiza
Menorca
Mallorca
Corse
Sardegna
Sicilia
Malta
Gibraltar
Andorra
San Marino
Monaco
Luxembourg
Liechtenstein
Vaduz
Cardiff
Birmingham
Manchester
Liverpool
Leeds
Glasgow
Edinburgh
Belfast
Cork
Galway
Limerick
Waterford
Kilkenny
Dublin
Kerry
Donegal
Sligo
Mayo
Clare
Kerry
Cork
Wexford
Wicklow
Kildare
Meath
Cavan
Monaghan
Fermanagh
Tyrone
Derry
Antrim
Down
Armagh
Leitrim
Roscommon
Galway
Mayo
Sligo
Donegal
Kerry
Cork
Waterford
Tipperary
Limerick
Clare

Cliquez sur une zone du dessin pour sélectionner une expérience

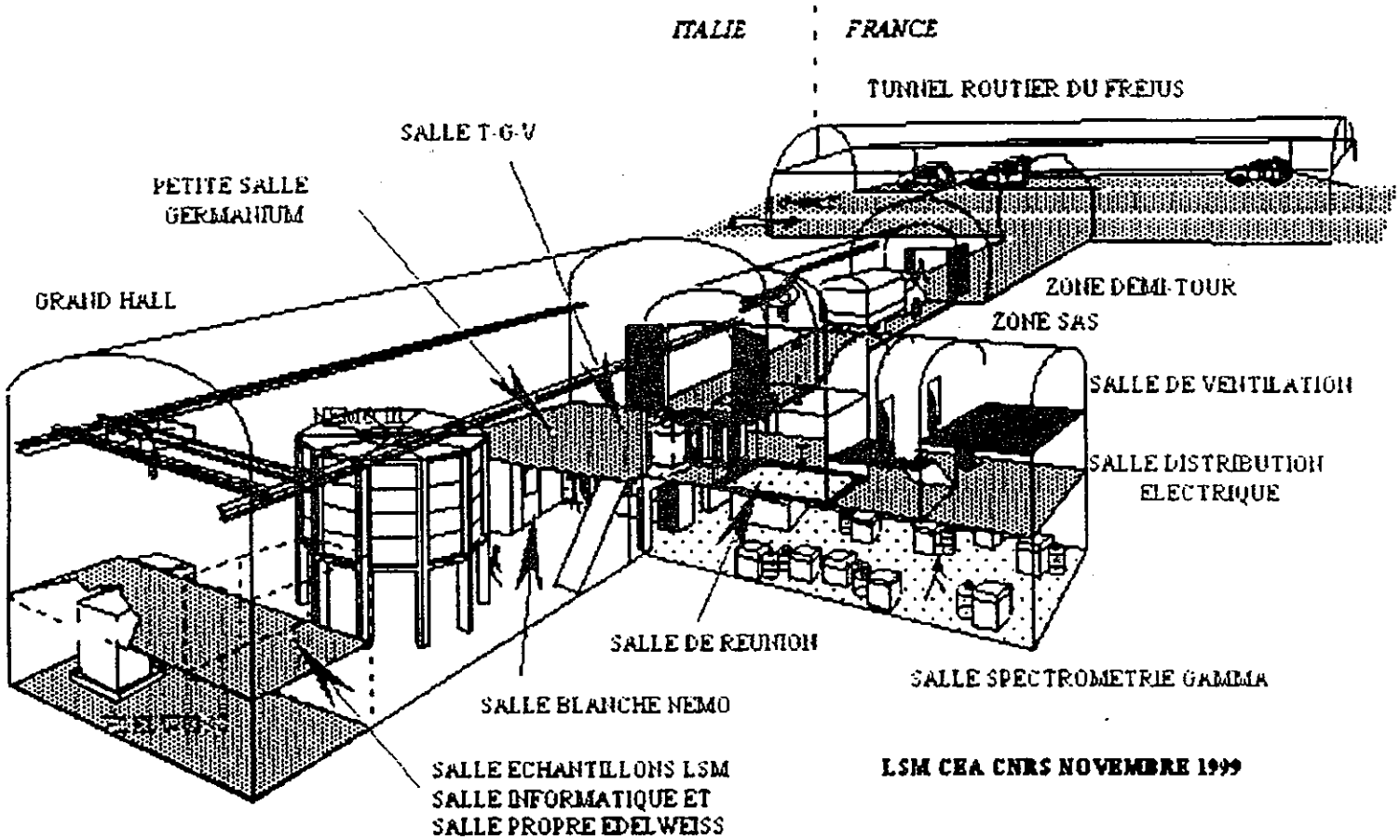

LSM
(Frejus)

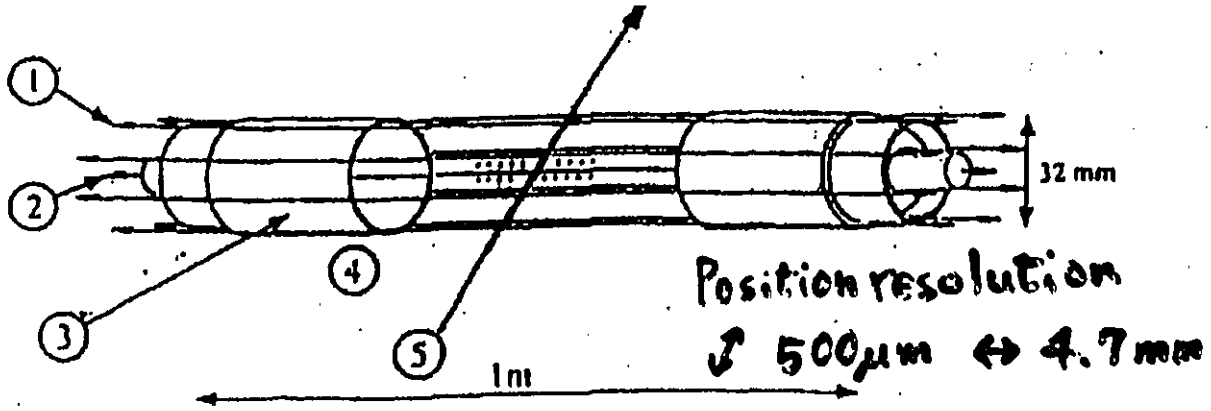

Fig. 3. Elementary Geiger cell. 1 – Eight grounded wires, diameter 100 μm, length = 1 m. 2 – Central anode wire, diameter 100 μm, length = 1 m, H.V. = +1800 V. 3 – Cathode ring (Ø = 29 mm). 4 – Helium gas (atmospheric pressure) + 4% ethyl alcohol. 5 – Through going particle and induced charges.

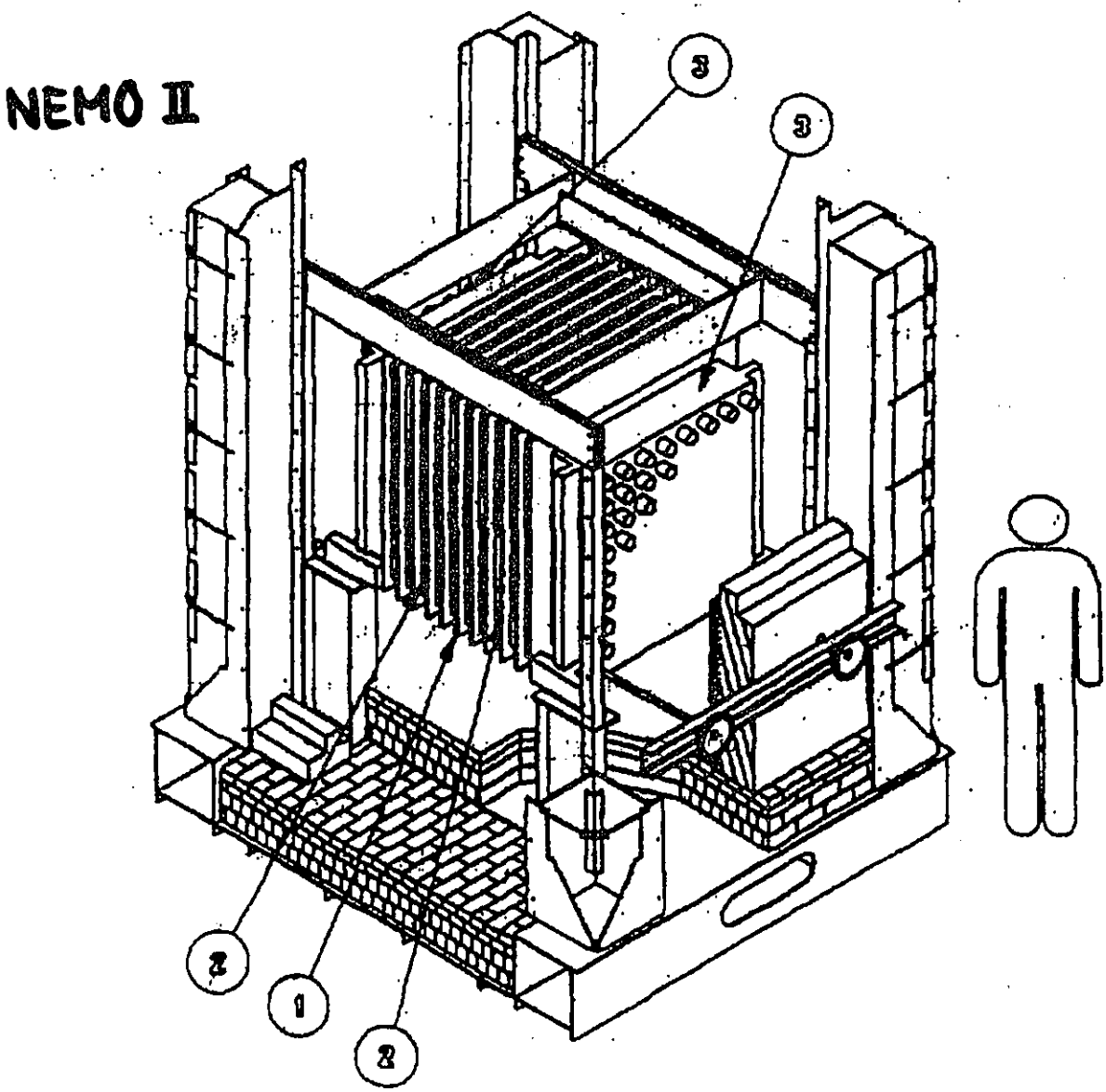

Fig. 2. Diagram of the experimental configuration. 1 – Central frame supporting the source. 2 – Copper frames which support the Geiger cells. 3 – 8×8 arrays of scintillator counters.

NEMO 2 ββ(2ν) RESULTS

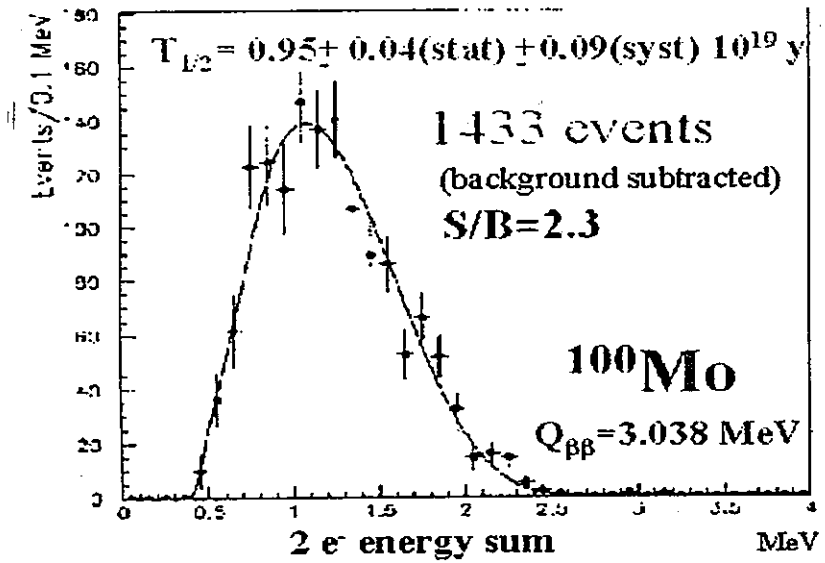

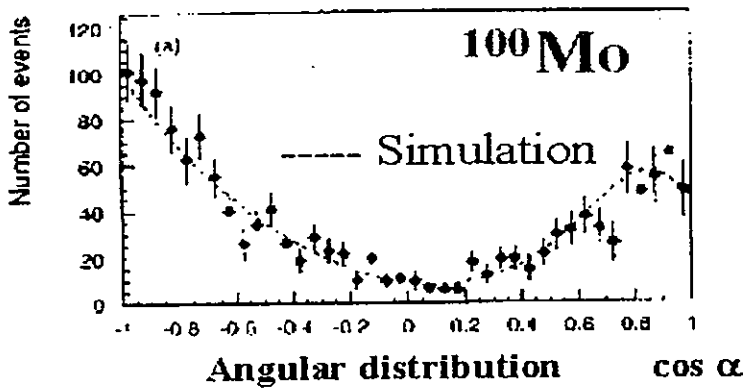

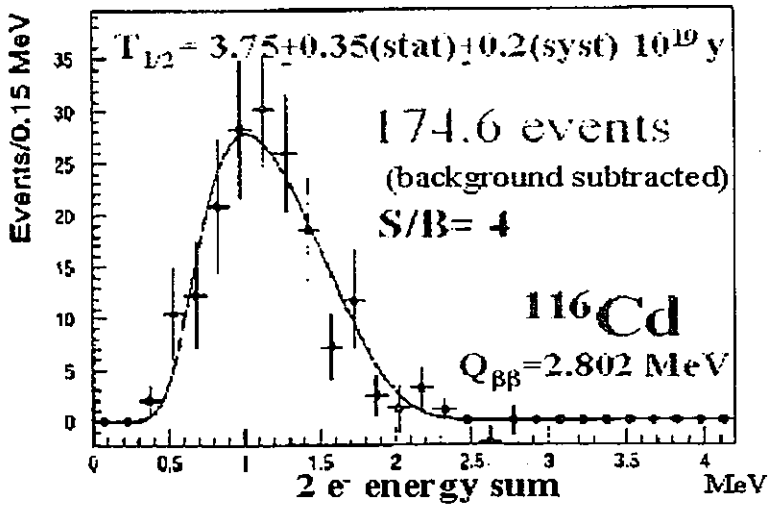

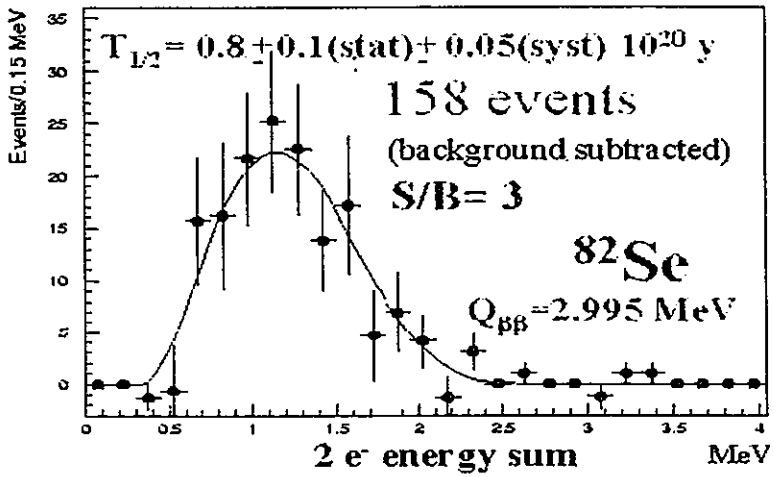

^{96}Zr $T_{1/2}$= $2.1^{+0.8}_{-0.4}$ ± 0.2(syst) 10^{19} y
$Q_{\beta\beta}$=3.350 MeV

Source distribution in NEMO3

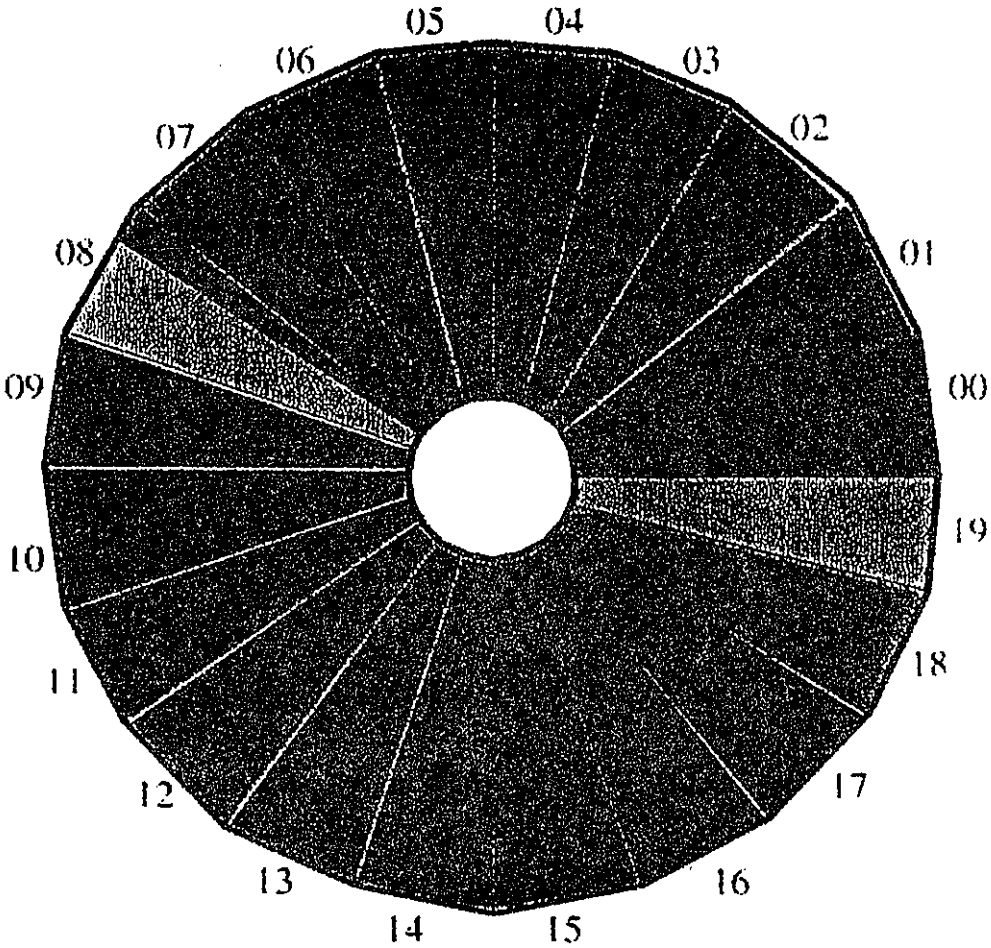

7 kg	^{100}Mo	12 sect.	}	2β2ν and 2β0ν
1 kg	^{82}Se	2.3 sect.		
0.6 kg	^{116}Cd	1 sect.		
0.9 kg	natFeO_2	1.7 sect.	}	background
1.7 kg	Cu	1 sect.		
0.7 kg	^{130}Te	≈ 1.5 sect.	}	2β2ν (2β0ν)
^{150}Nd, ^{96}Zr, ^{48}Ca		≈ 0.5 sect.		
50 g	16 g	8 g		

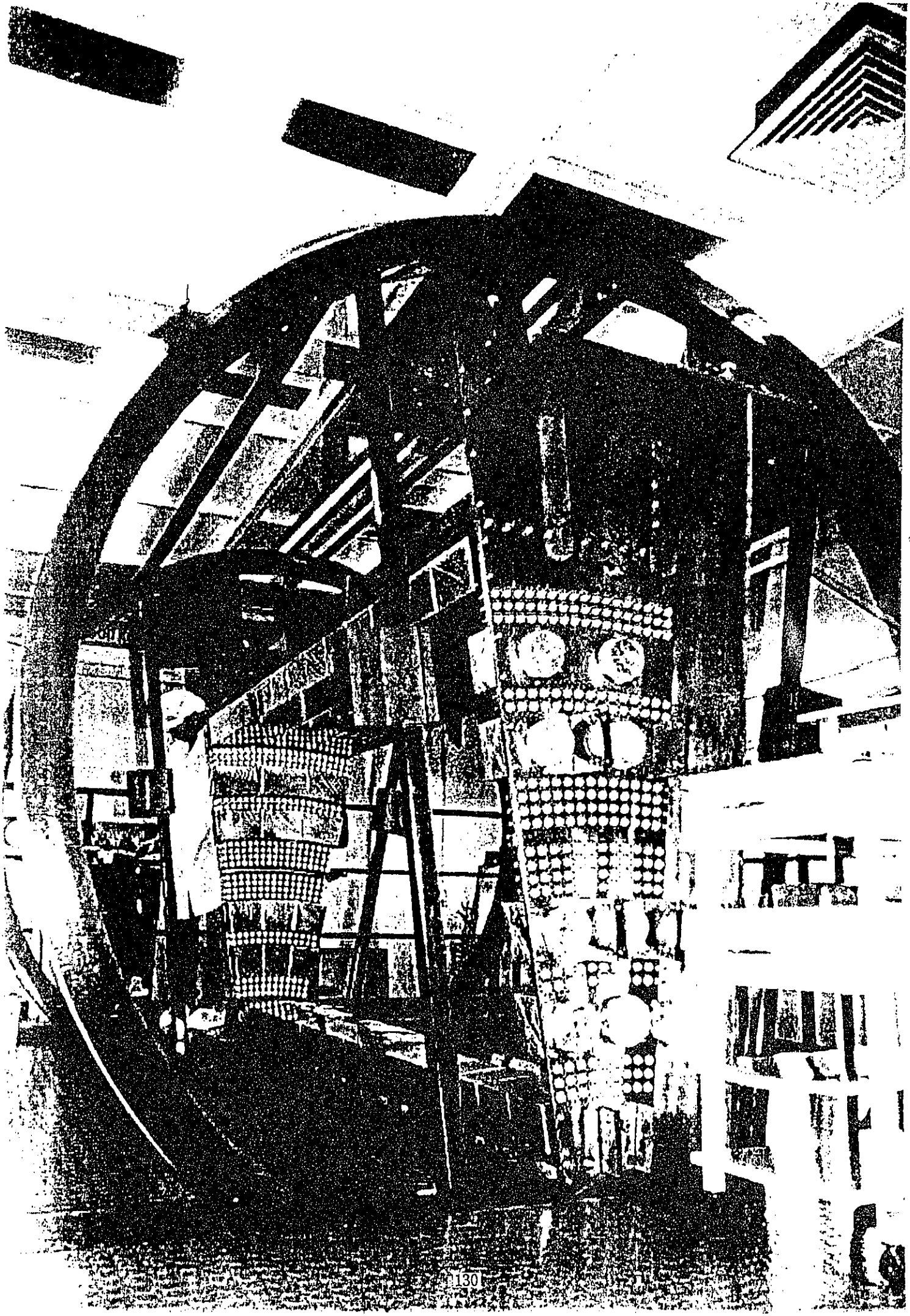

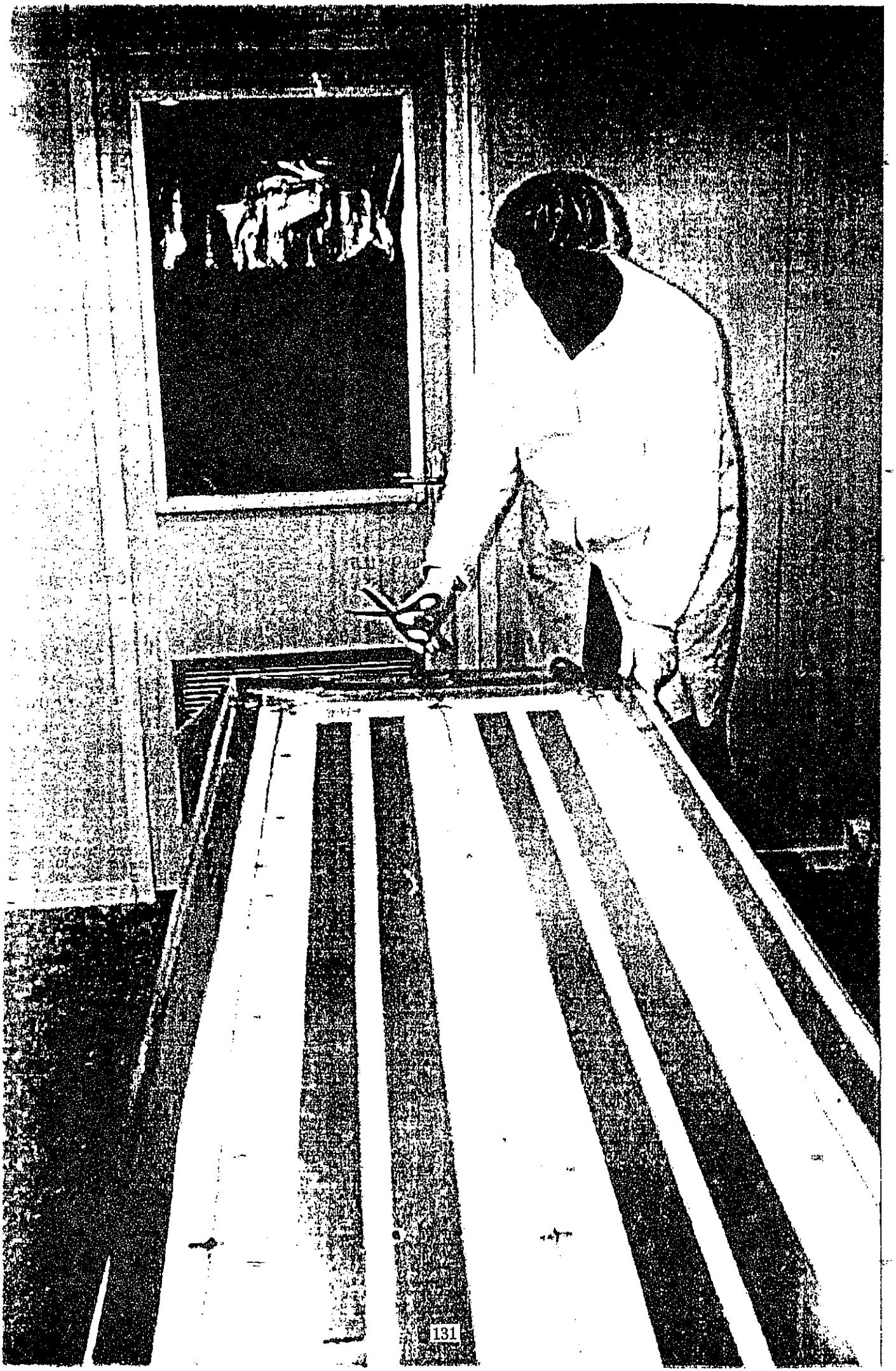

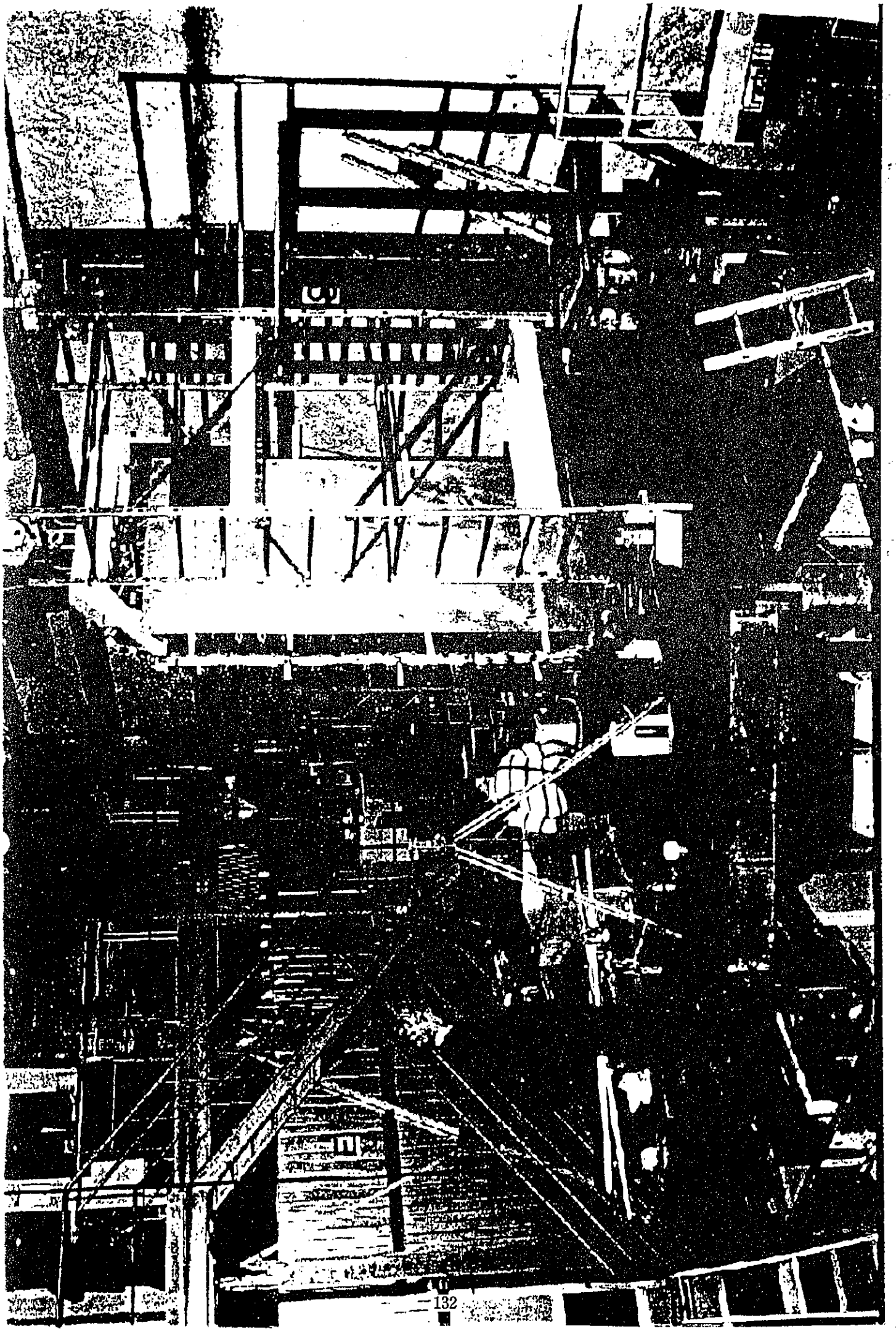

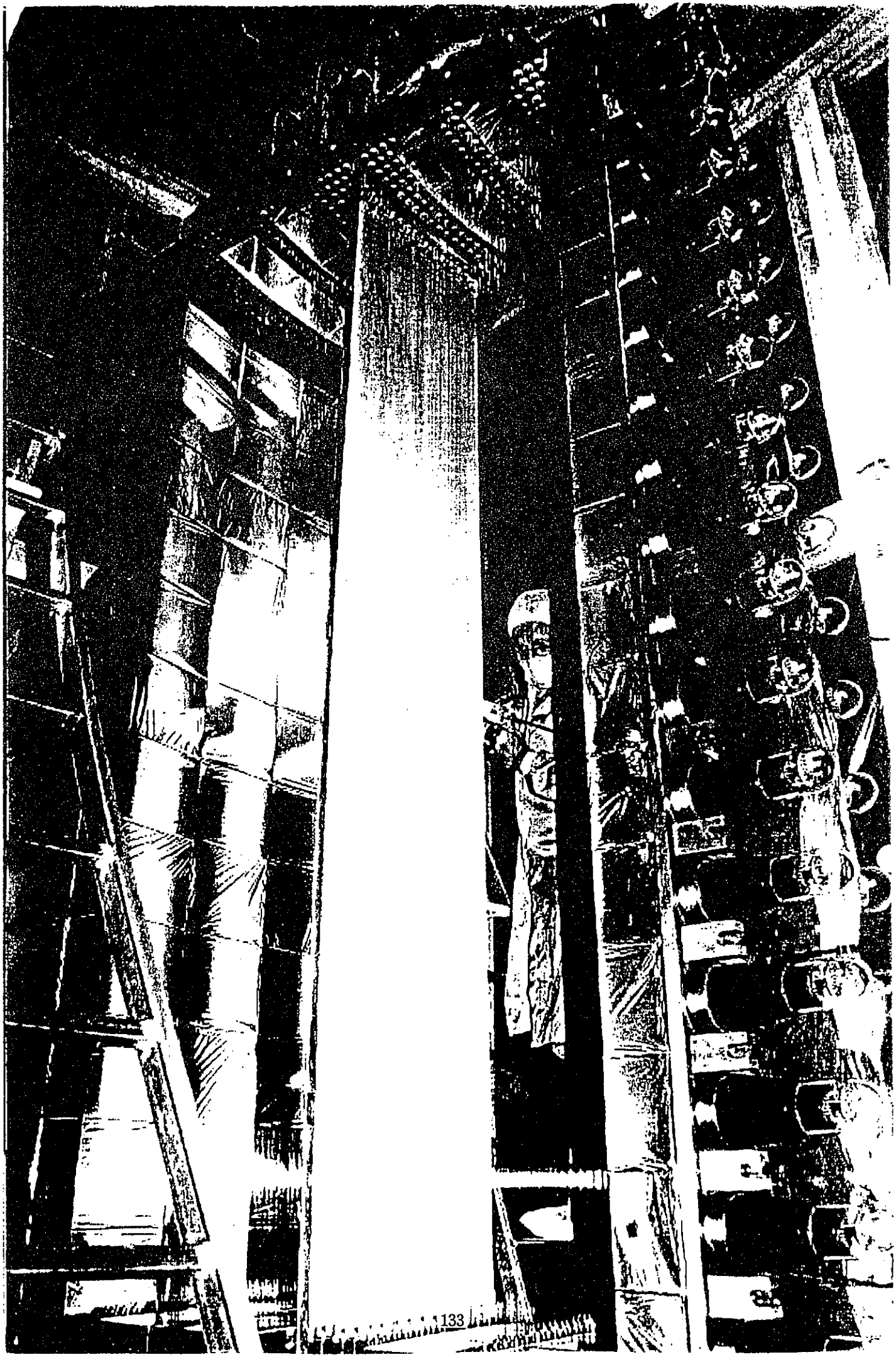

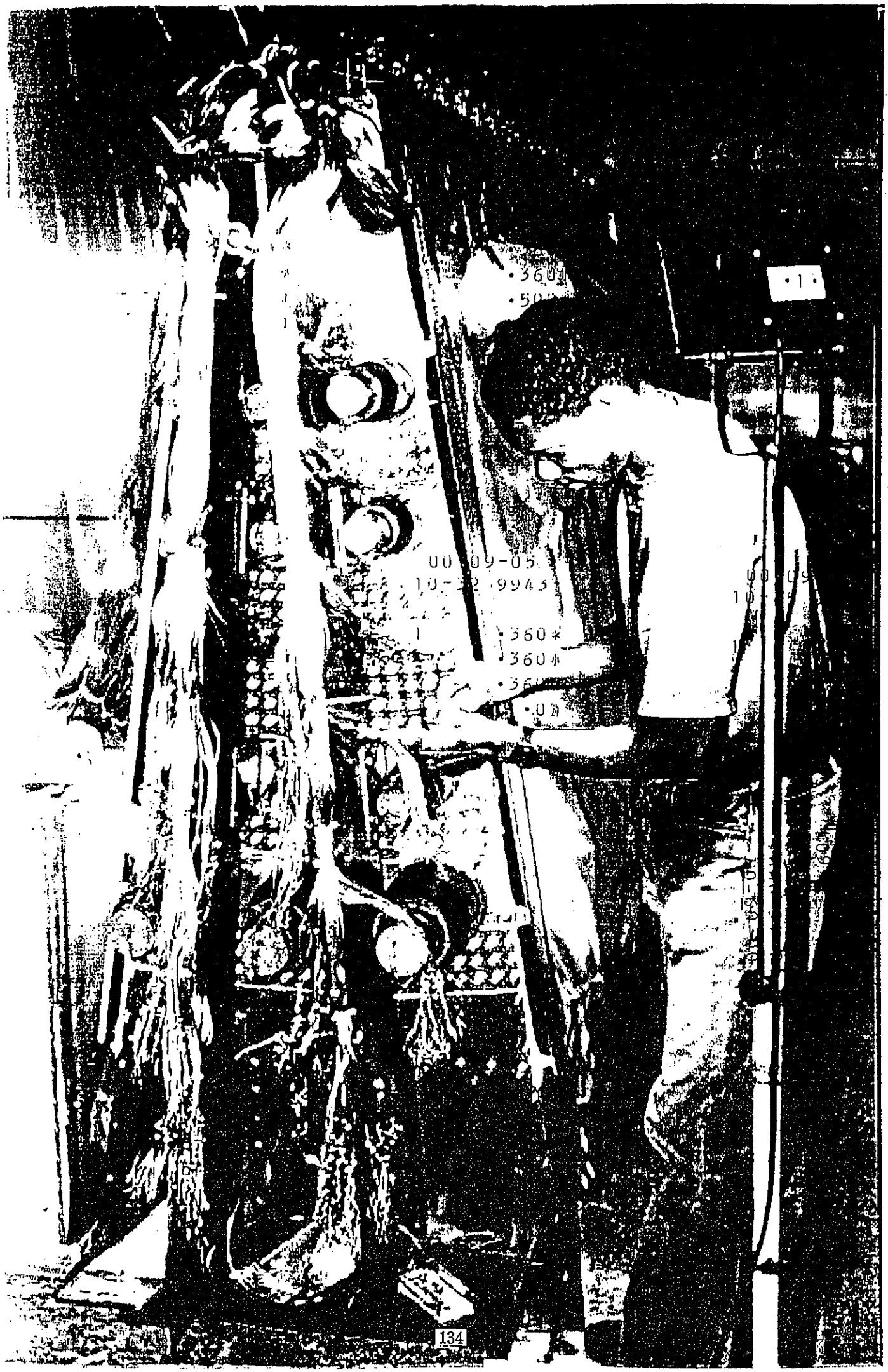

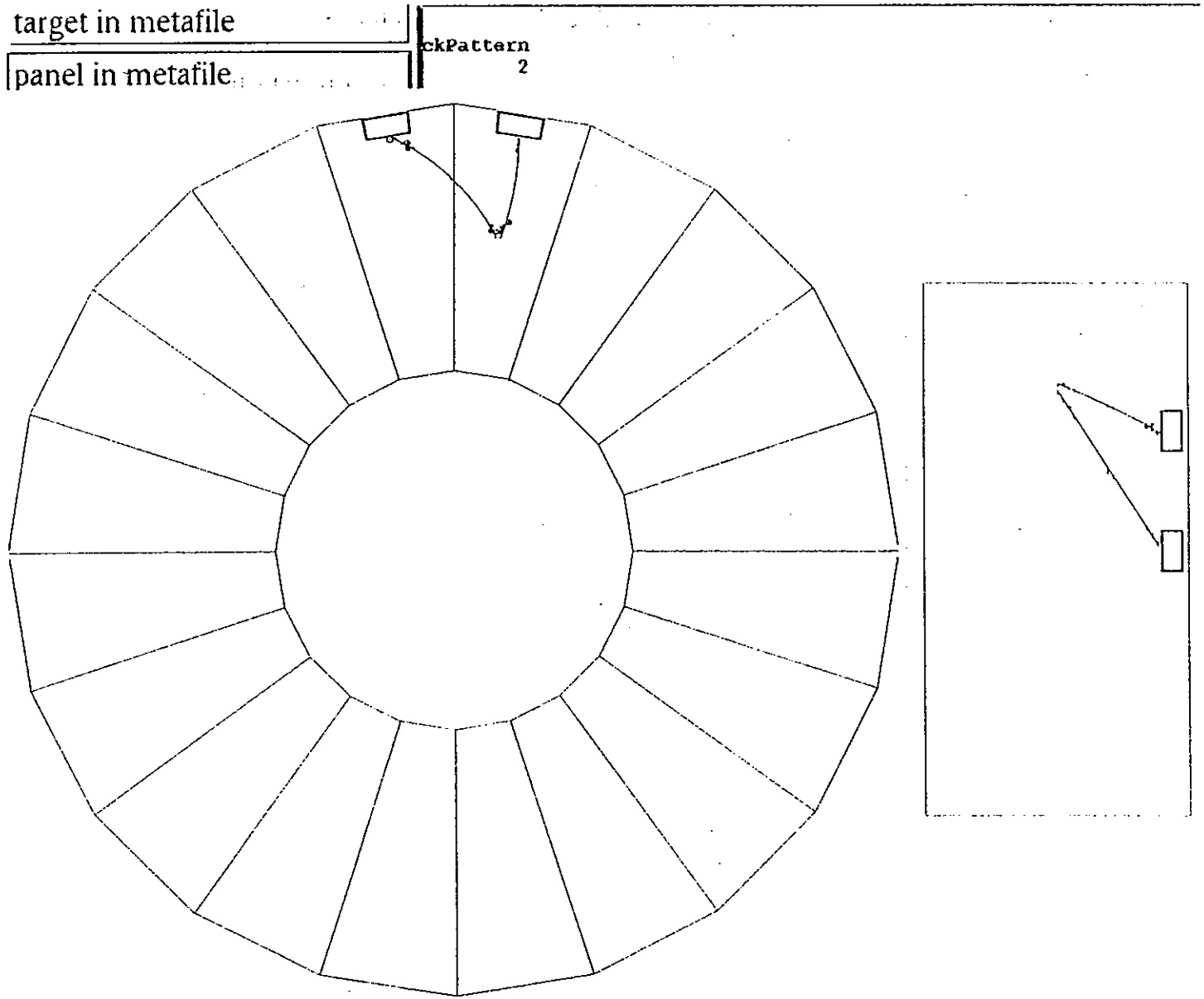

fig/ev fig

Background in the ββ(0ν) region

Signal

$Q_{\beta\beta}$ ^{100}Mo=3.038 MeV

Internal background

Source contaminations
^{214}Bi (Q_β=3.3 MeV)
^{208}Tl (Q_β=5.0 MeV)

ββ(2ν) decay

External background

Interaction of γ rays produced by *neutrons* captures

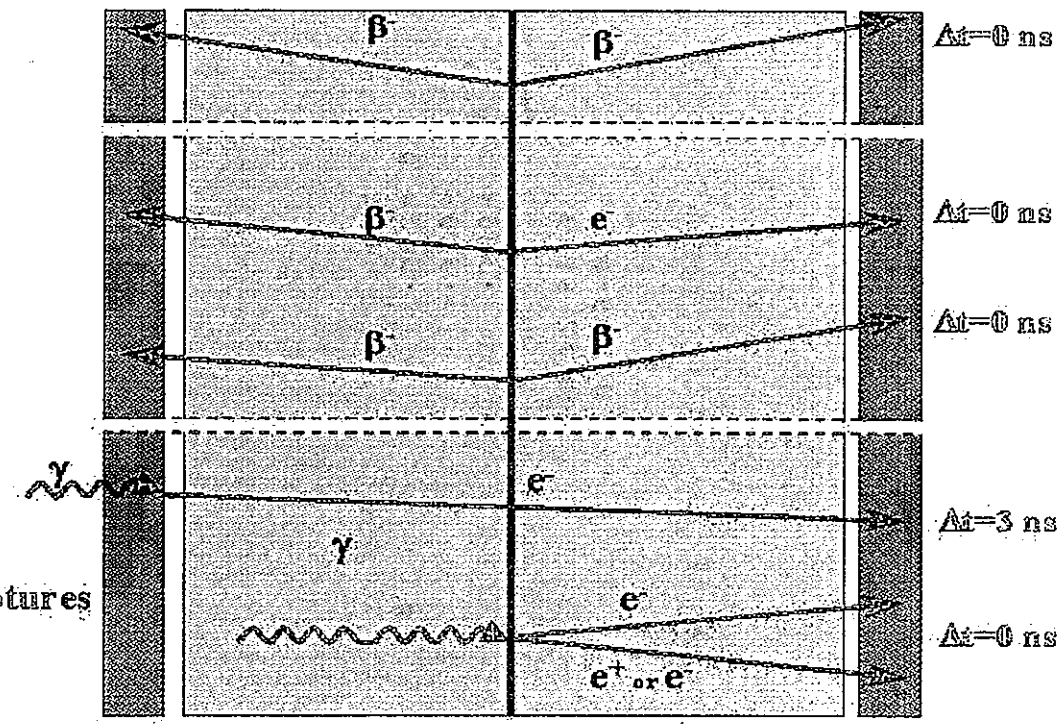

e⁺e pairs
Double Compton
Compton + Möller

In the Frejus underground laboratory:
Fast neutron flux (> 1 MeV): 3.5 ± 1.5 10^{-6} $n.cm^{-2}s^{-1}$
Thermal neutron flux (~0.025 eV) : 1.6 ± 0.1 10^{-6} $n.cm^{-2}s^{-1}$

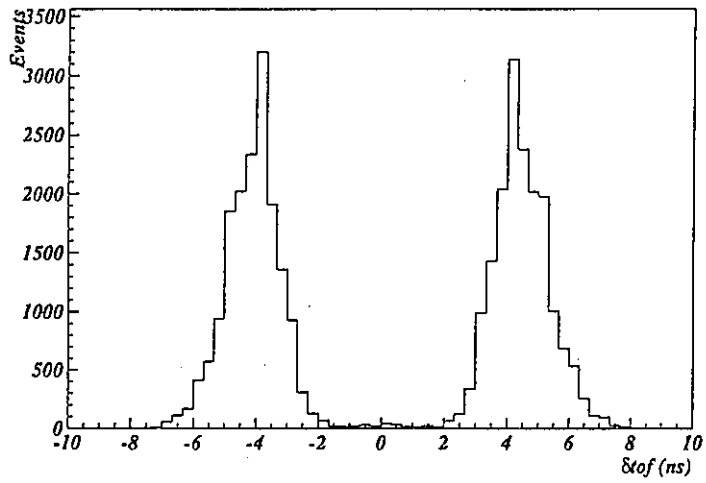

Fig. 3. Distribution of experimental times of flight for both "two electron" events (centered around 0 ns) and "one crossing electron" events (centered around 4 and -4 ns) obtained during 10700 h.

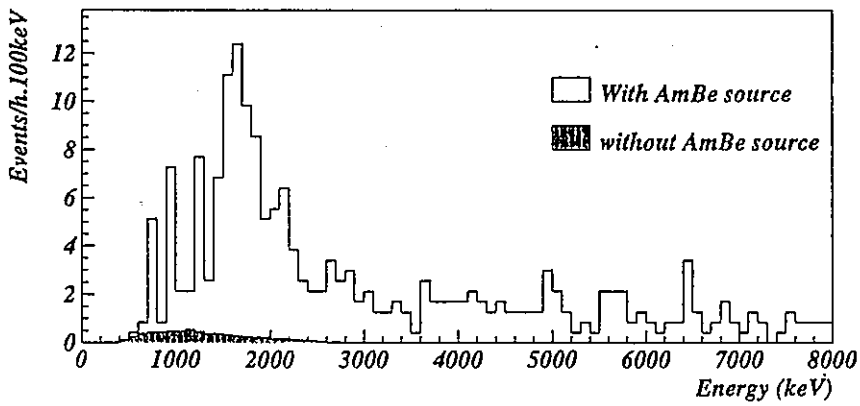

Fig. 4. Energy sum of "one crossing electron" events recorded during 1 h with and without neutrons source.

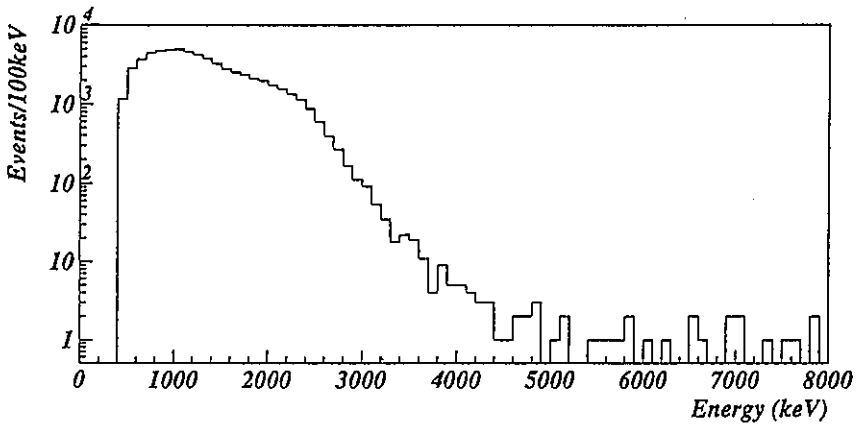

Fig. 7. Energy spectrum of "one crossing electron" events recorded during 10700 hours (for the four shielding configurations) with the NEMO 2 prototype

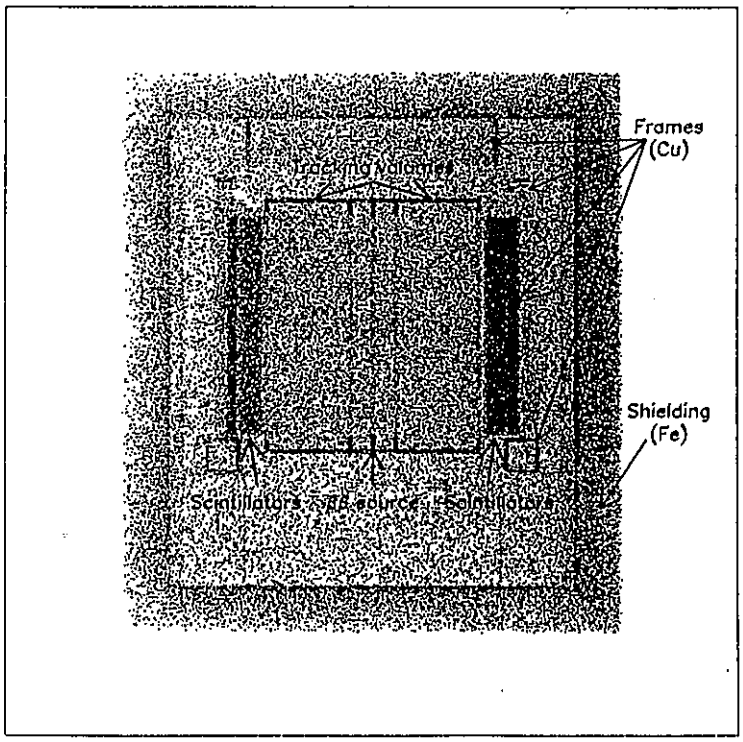

Fig. 8. Projection of the simulated neutron capture places in the NEMO 2 detector in the case of the neutron source located in the south side of the NEMO 2 prototype.

n/γ Background Simulations

GEANT/MICAP + New library for γ-emission after neutron capture and scattering

5" R6594 (385g)
K-40 0.53 Bq/PMT
Bi-214 0.24 Bq/PMT
Tl-208 0.014 Bq/PMT

3" R6091 (230g)
K-40 0.34 Bq/PMT
Bi-214 0.083 Bq/PMT
Tl-208 0.005 Bq/PMT

Mo source foil < 0.2 mBq/kg (^{214}Bi) < 0.01 mBq/kg (^{208}Tl)

Components	Weight (kg)	Total Activity (in Bq) ^{40}K	^{214}Bi	^{208}Tl	^{60}Co
PMTs	600	830	300	18	
scintil.	5,000	<100	<0.7	<0.3	1.8 ± 0.4
copper	25,000	<125	<25	<10	<6
petals iron	10,000	<50	<6	<8	17 ± 4
μ metal	2,000	<17	<2	2.0 ± 0.7	4.3 ± 0.7
wires	1.7	$<8.10^{-3}$	$<10^{-3}$	$<6.10^{-4}$	10^{-2}
shield. iron	180,000	<3000	<300	<300	300 ± 100

Table 1: Total activities (in Bq) for the main components of the NEMO-3 detector, measured with HP-Ge detectors in the Fréjus Underground Laboratory.

γ Source Candidates:
(energy beyond well known region) (E>3MeV)

- Cosmic μ ($\geq$ TeV) Bremsstrahlung (no μ-capture)

  (wide energy region)

- Neutron capture γ-ray

  1. $\Leftarrow$ outside surrounding materials ... I_γ
  2. $\Leftarrow$ inside the detector itself ... I_n

$\Sigma E_\gamma \sim 8MeV$ (6.5 - 10MeV)

which corresponds to the neutron binding energy.

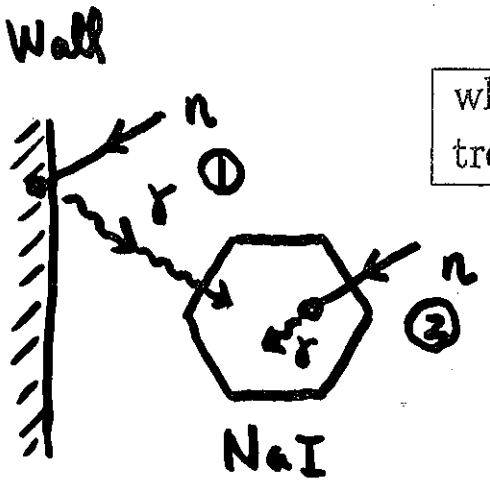

The Energy Spectrum of NaI detector (in LSM)

1 bin = 20 keV 7554 hours (Normalize)

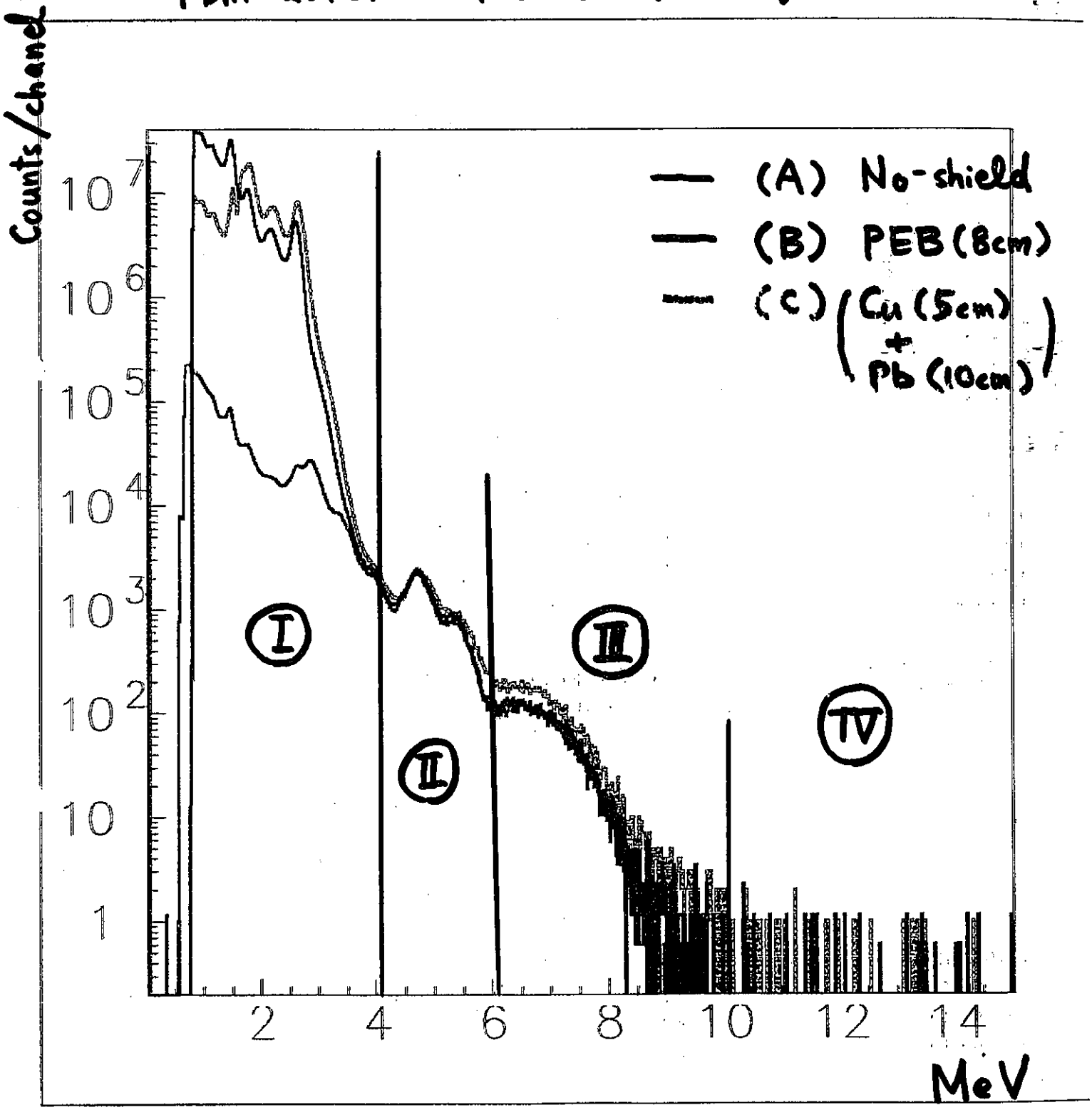

Results (preliminary)

1. Region III: (6 MeV $\leq$ E $\leq$ 10 MeV)
   - $I_\gamma(6-10MeV) = 3.2(\pm 1.0) \cdot 10^{-6}/\mathrm{cm}^2/\mathrm{sec}$
   - $I_n(\mathrm{capture(NaI,Cu)}) = 2 \sim 7 \cdot 10^{-6}/\mathrm{cm}^2/\mathrm{sec}$ →
2. Region II+III: (4 MeV $\leq$ E $\leq$ 10 MeV)
   - $I_\gamma(4-10MeV) \sim 7 \cdot 10^{-6}/\mathrm{cm}^2/\mathrm{sec}$
3. Region IV: (E $\geq$ 10 MeV)
   - Direct effect:
     $I_\mu = (9 \pm 4) \times 10^{-9}/\mathrm{cm}^2/\mathrm{sec}$ ($\Rightarrow 7.7 \pm 4.4/\mathrm{m}^2/\mathrm{day}$)
     (cf. 4 /m^2/day Frejus exp.)
     (cf $1.75 \cdot 10^{-2}/\mathrm{cm}^2/\mathrm{sec}$ at Bordeaux)
   - μ Bremsstrahlung:
     $I_\gamma(E \geq 10MeV) \sim 1.0 \pm 0.3 \cdot 10^{-8}/\mathrm{cm}^2/\mathrm{sec}$

$I_{thermal}$ ($\simeq$ 0.025eV)
$= 1.6 \pm 0.1 \cdot 10^{-6}$ n/cm^2/sec

V. Chazal. et al Astroparticle Physics

^{3}He counter

NEMO 3 : Expected performances

- ***10 kg of ^{100}Mo*** *($Q_{\beta\beta}$ = 3.038 MeV) -* ***5 years***
- *Source contamination:* $^{214}Bi < 0.3$ *mBq/kg*
  $^{208}Tl < 0.02$ *mBq/kg*
- *$\vec{B}$=30 Gauss + (20 cm iron + 20 cm paraffin) shielding*

⇓

Internal Background:	< 0.16 (TOTAL)		5 year · 10 kg < 9
^{208}Tl	< 0.04	events/y/kg	< 2
^{214}Bi	< 0.03	events/y/kg	< 1.5
$\beta\beta(2\nu)$	0.11	events/y/kg	5.5
External Background:			
	< 0.01	events/y/kg	≤ ~~0.05~~ 0.5

9.5 background events expected in 5 years

Signal (5 σ effect) ⇙ ⇘ **Limit (90 % CL)**

24 events detected ⇓ $T_{1/2} = 3.5\ 10^{24}$ y ⇓ $\langle m_\nu \rangle = 0.3 - 0.7$ eV

6 events excluded ⇓ $T_{1/2} > 9.\ 10^{24}$ y ⇓ $\langle m_\nu \rangle < 0.2 - 0.5$ eV

Thermal Detectors (Bolometers)

$$\Delta T = \frac{Q}{C_v}$$

$$C_v = 1944 \left(\frac{V}{V_m}\right)\left(\frac{T}{\Theta}\right)^3 \ J/K$$

$$\Delta E \simeq \sqrt{k C_v T^2}$$ ($\Delta E \sim 100\,eV$ 1 MeV
Ge 1 kg 10 mK)

Possible Detectors for $\beta\beta$ decays

TeO_2, CaF_2, Ge, $CdWO_4$, $^{100}MoPbO_4$,

CUORE (Cryogenic Underground Observatory for Rare Events)

① Present 1 crystal × 20 = 6.8 kg (34% ^{130}Te 2.3 kg)
= 340 g

② CUORICINO 4 crystal × 14 plane = 56 Crystal
42 kg (^{130}Te 13.3 kg)

③ CUORE 4 × 15 × 17 tower = 1020
775 kg (^{130}Te 210 kg)

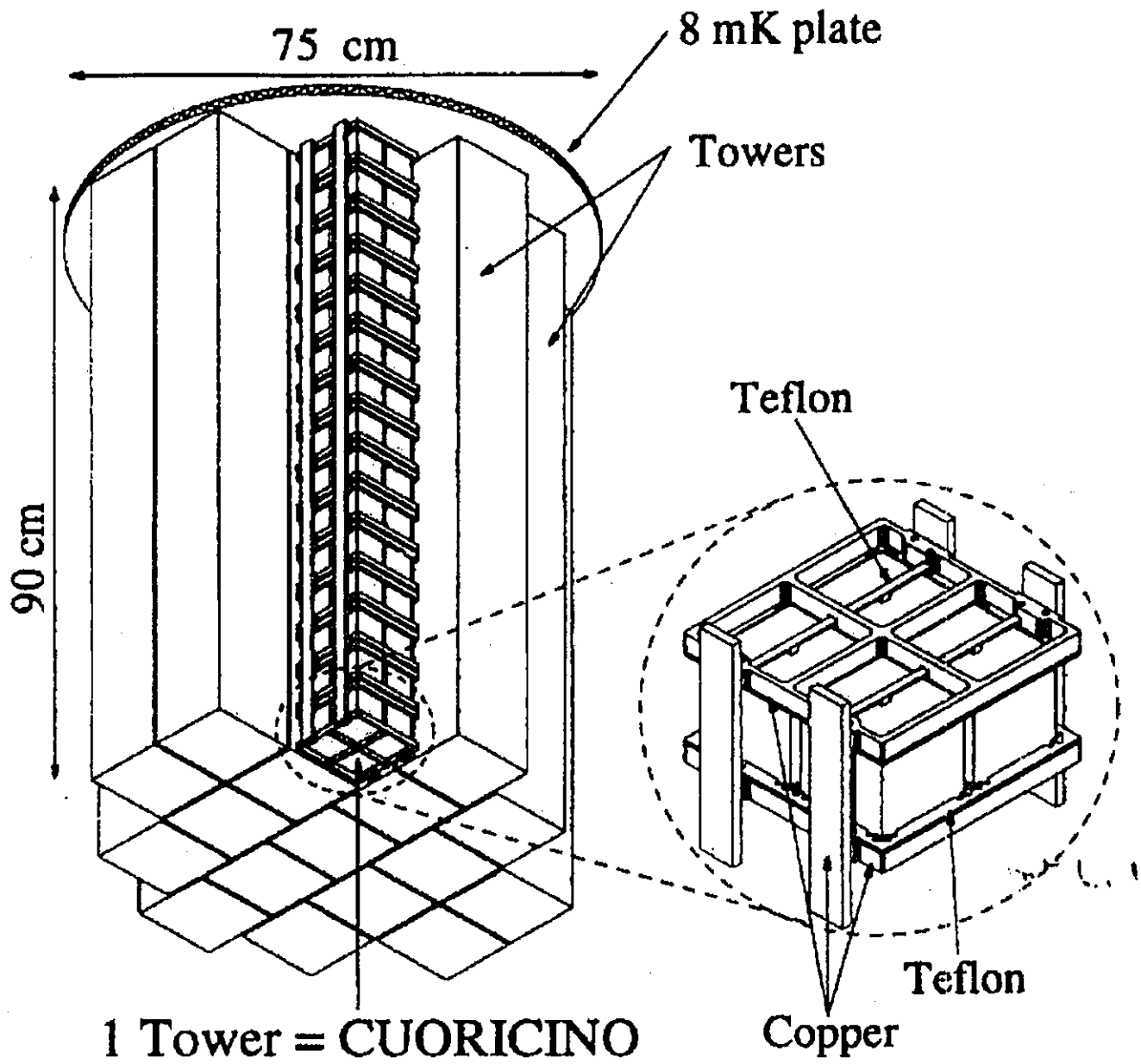

Figure 1. Preliminary CUORE design

DCBA

Drift Chamber Beta Analyzer

- DC 46.5 × 52.4 × 68.0 cm^3
- B solenoid ~0.8kG
- ^{150}Nd (source canbe easily changed)

^{48}Ca by ELEGANT VI

CaF_2 @ Oto, Nara

^{48}Ca 62g (1.3 mol) in CaF_2

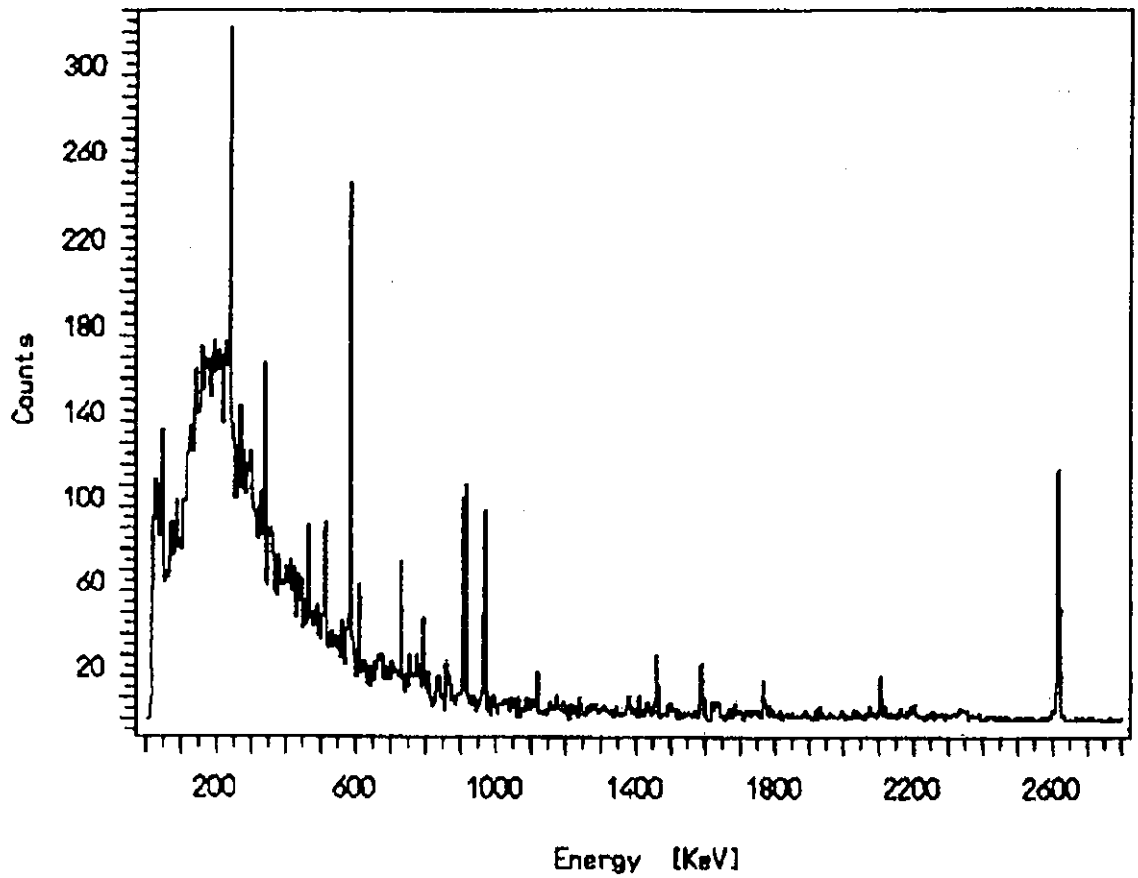

Figure 2. Calibration spectrum of a 750 g crystal

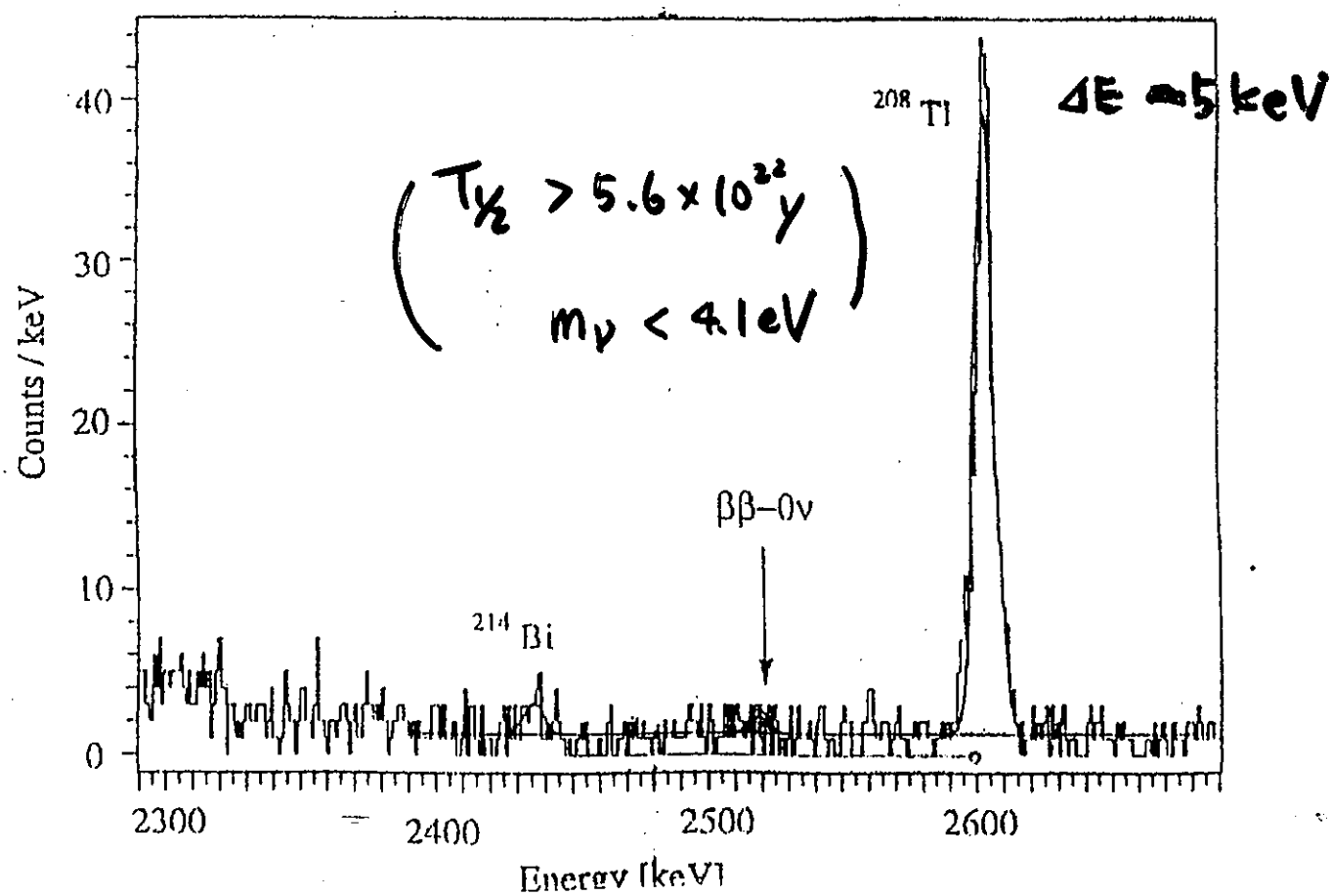

CUORICINO set-up

The CUORICINO array is a set of

56 cubic TeO_2 crystals of 5 cm side and 760 g mass

arranged in a tower-like structure of

14 planes with 4 crystals per plane

The gap between the crystals is only 6 mm

compact structure which helps in study and reduction of background through coincidence analysis

SINGLE CUORICINO PLANE: now under test

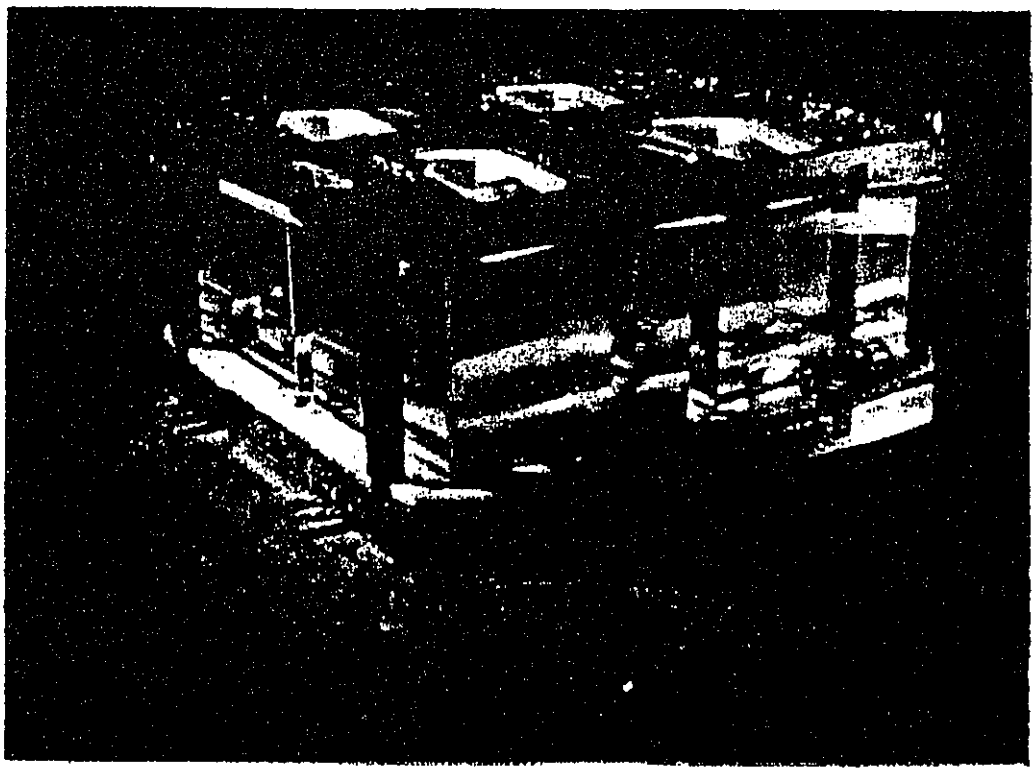

Xe in liquid scintillators

^{136}Xe (8.9% → 80%)
easily enriched

Xe ··· 2.14% solubility 15°C 900 mbar

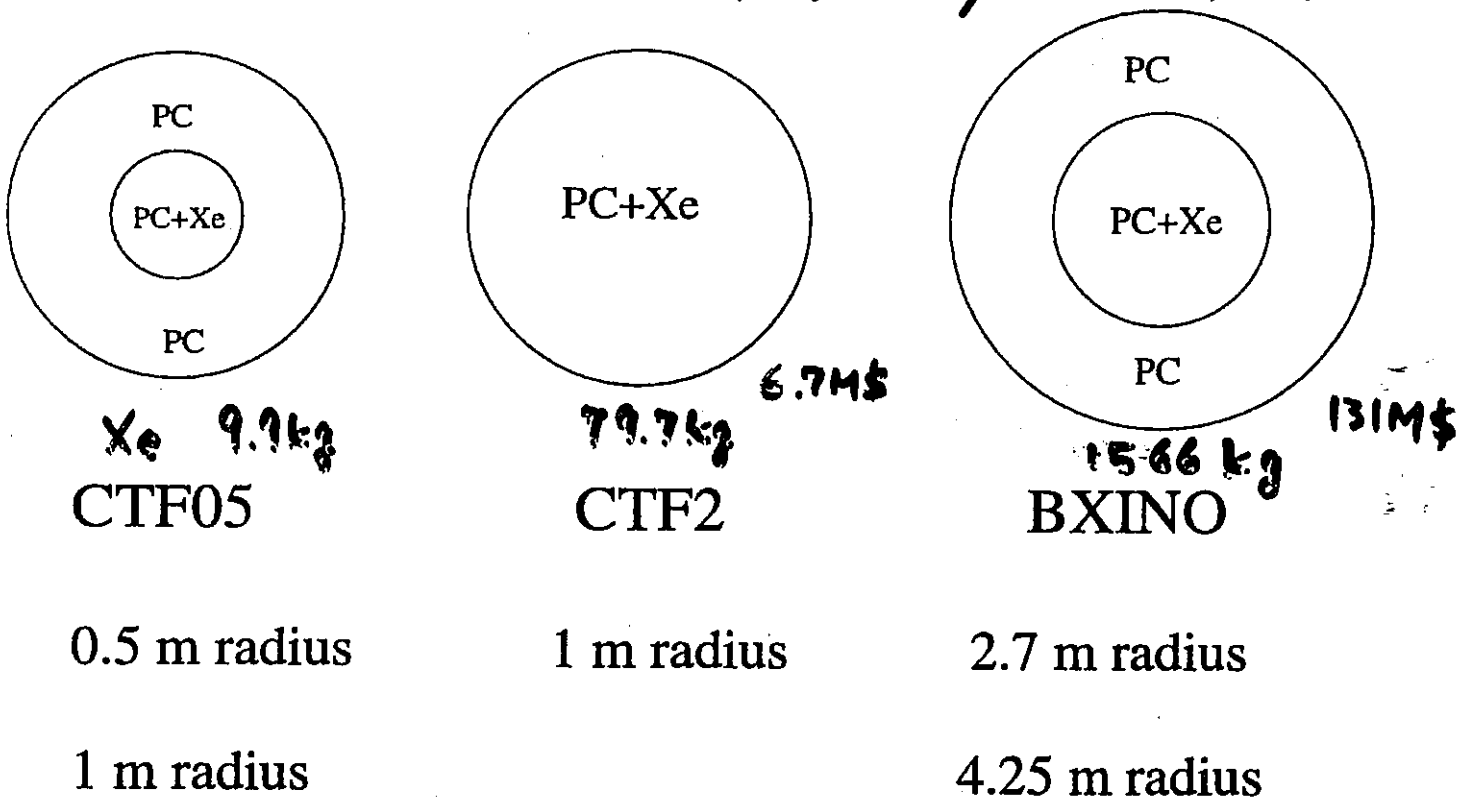

Fig. 4. Geometrical features of the three considered configurations. The CTF2 configuration is the same as the CTF, with the scintillator loaded with xenon. On the contrary, the CTF05 and BOREXINO (BXINO) configurations feature an innerinner vessel which contains the PC + Xe solution, whereas the rest of the inner vessel contains PC alone.

PC: PC+PPO liquid scintillator

cf

(LENS 20 ton Yb

$^{176}Yb \rightarrow {}^{176}Hf + 2\beta^- (+2\bar{\nu}_e)$

12.7% Q = 1085.5 keV)

CAMEO

Ⓘ ^{100}Mo, ^{116}Cd, ^{82}Se, ^{150}Nd (~1kg

Φ = 180cm disk in BOREXINO CTF

Ⓘⓘ $^{116}CdWO_4$ (65 kg)
(as scintillating crystals)
(in BOREXINO)

Ⓘⓘⓘ $^{116}CdWO_4$ 1 ton

TABLE I. Liquid Xenon as a WIMP Detector.

1. Large mass available - up to tons.
   - Atomic mass: 131.29
   - Density: 3.057 gm/cm^3
   - W_i value (eV/pair) 15.6 eV
   - No long-lived isotopes of xenon

2. Drift velocity: 1.7 mm/μs
   - 250 V/cm
   - Scintillation wave length: 175 nm
   - Decay time: 2 ns → 27 ns

3. Light yield > NaI, but intrinsic scintillator (no doping)

⇒ Excimer process very sell understood
⇒ First excimer laser was liquid xenon in 1970!

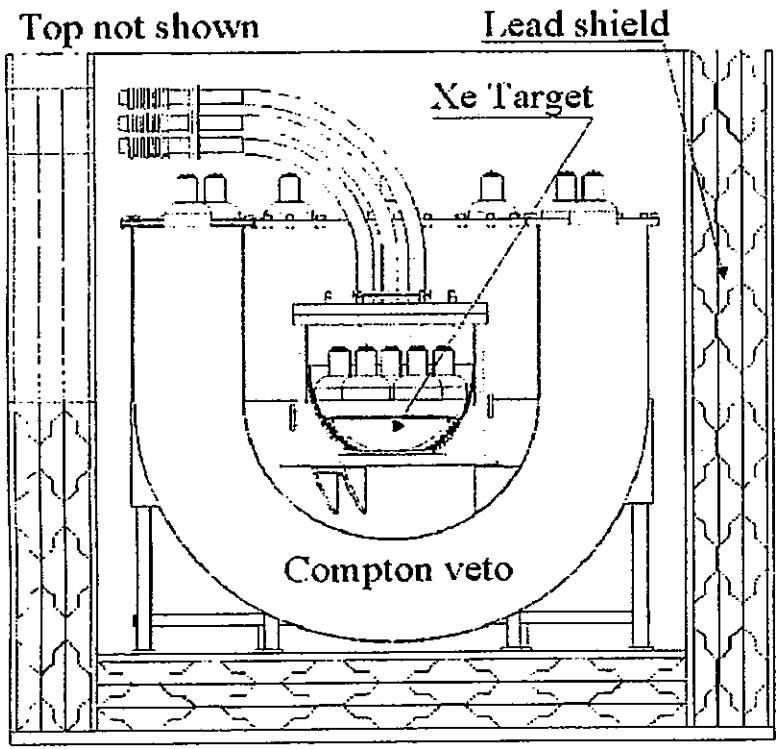

(A)

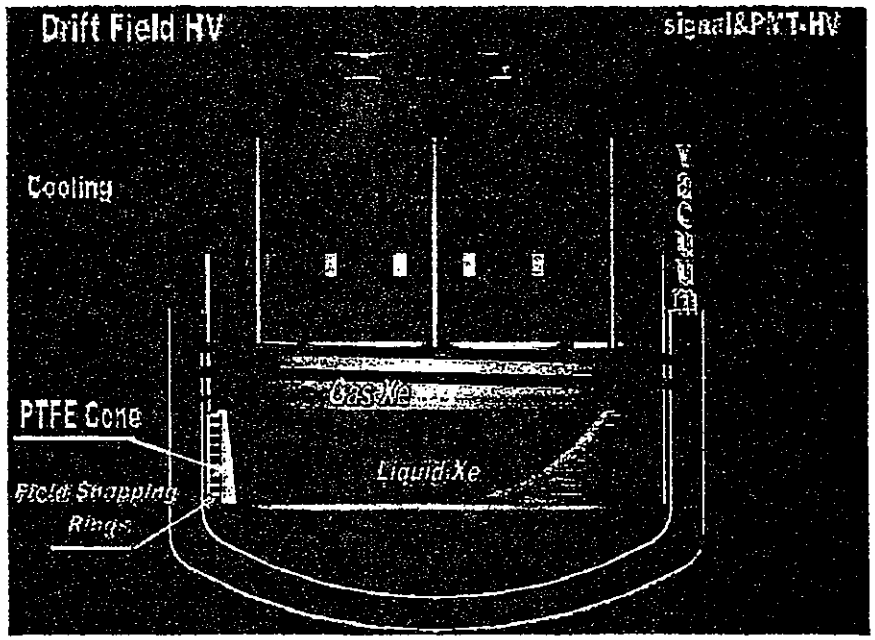

(B)

FIGURE 5. System setup for Xe target (40 kg total): (A) Overall set up and (B) ZEPLIN II central detector.

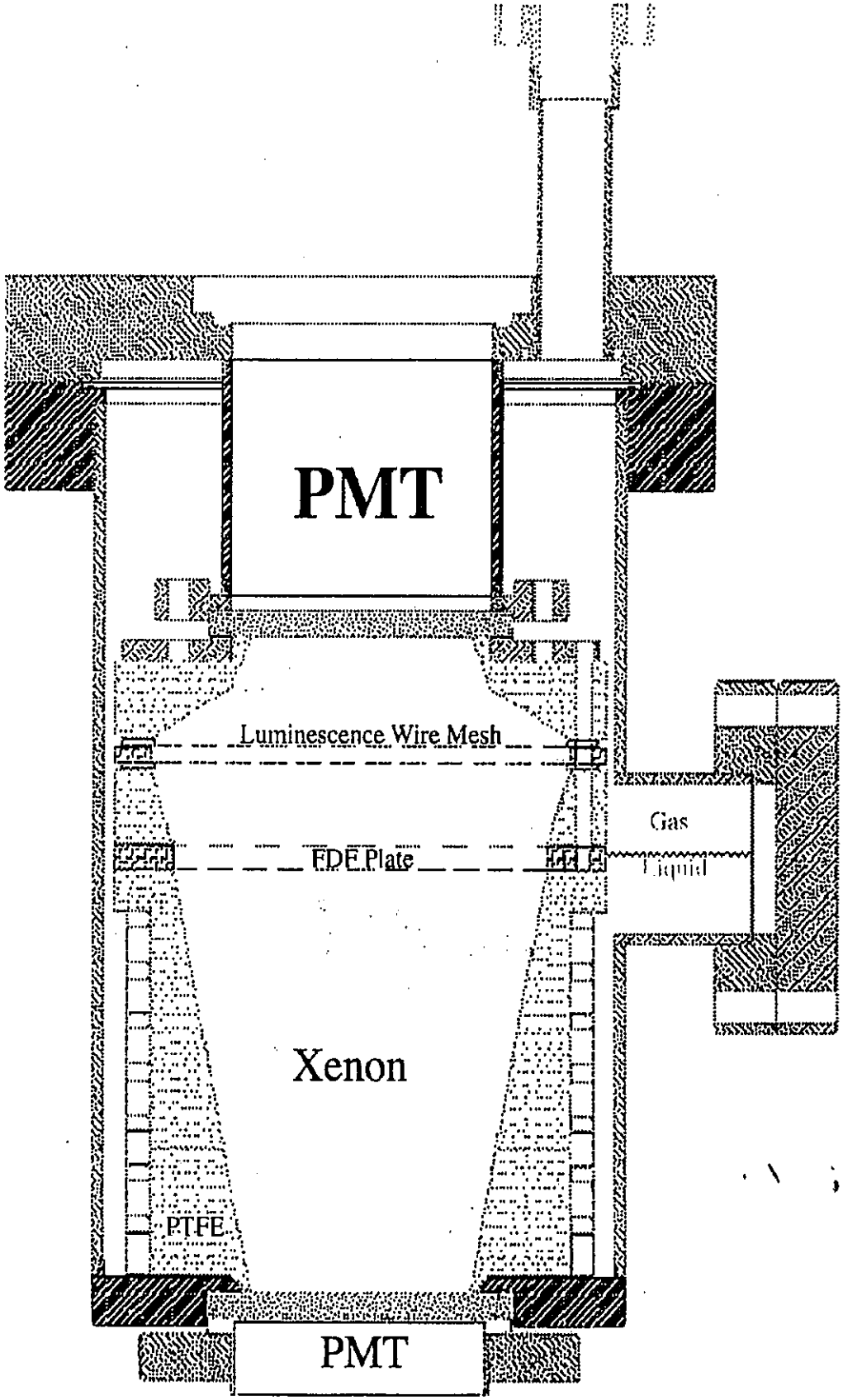

FIGURE 3. XEPLIN II: Electroluminescence in gas (principle of a two-phase, 1-kg detector, developed by UCLA–CERN–Torino).
photons